Award Number: W81XWH-16-1-0189

TITLE: Compensatory Immune Suppression Following PD-1/PD-l1 Checkpoint Blockade in Ovarian Cancer

PRINCIPAL INVESTIGATOR: Keith L Knutson

CONTRACTING ORGANIZATION: MAYO CLINIC
JACKSONVILLE, FL 32224

REPORT DATE: DECEMBER 2018

TYPE OF REPORT: Final report

PREPARED FOR: U.S. Army Medical Research and Materiel Command
Fort Detrick, Maryland 21702-5012

DISTRIBUTION STATEMENT: Approved for Public Release; Distribution Unlimited

REPORT DOCUMENTATION PAGE	*Form Approved OMB No. 0704-0188*

1. REPORT DATE	**2. REPORT TYPE**	**3. DATES COVERED**
DECEMBER 2018	Final	1Sept2016 - 31Aug2018

4. TITLE AND SUBTITLE **Compensatory Immune Suppression Following PD-1/PD-l1 Checkpoint Blockade in Ovarian Cancer**	**5a. CONTRACT NUMBER** W81XWH-16-1-0189 **5b. GRANT NUMBER** W81XWH-16-1-0189 **5c. PROGRAM ELEMENT NUMBER**
6. AUTHOR(S) Keith L Knutson E-Mail: Knutson.Keith@mayo.edu	**5d. PROJECT NUMBER** **5e. TASK NUMBER** **5f. WORK UNIT NUMBER**
7. PERFORMING ORGANIZATION NAME(S) AND ADDRESS(ES) Mayo Clinic, Department of Immunology, Mayo Clinic Florida 4500 San Pablo Rd. Jacksonville, FL 32224	**8. PERFORMING ORGANIZATION REPORT NUMBER**
9. SPONSORING / MONITORING AGENCY NAME(S) AND ADDRESS(ES) U.S. Army Medical Research and Materiel Command Fort Detrick, Maryland 21702-5012	**10. SPONSOR/MONITOR'S ACRONYM(S)** **11. NUMBER(S)**

12. DISTRIBUTION / AVAILABILITY STATEMENT
Approved for Public Release; Distribution Unlimited

13. SUPPLEMENTARY NOTES

14. ABSTRACT

Ovarian cancer (OC) is highly immunogenic and generally speaking, higher lymphocytic infiltration is associated with better outcomes. Despite the presence of anti-tumor immune effectors, OCs overcome the immunologic onslaught by complex immune suppression strategies involving infiltration by a variety of specialized lymphoid or myeloid derived suppressor or regulatory cells and/or the direct production and release of factors by the tumor into the tumor microenvironment. PD-1 and its ligands PD-L1 and PD-L2 constitute an important immune regulatory (i.e. checkpoint) pathway which suppresses or impairs effective T, B, and myeloid cell responses both in the initiation and effector phases of the immune response. This regulatory axis is widely thought to be important preventing autoimmunity during traditional immune responses, such as against infectious agents. Tumor regressions in response to PD-1/PD-L1 blockade constitute a major fraction of the objective responses (which include disease stabilizations and minor regressions) suggesting that there are biologic subsets of tumors that are more amendable to checkpoint blockade or, alternatively, tumors rapidly upregulate compensatory immune suppression mechanisms following exposure to checkpoint blockade that prevent their destruction.

15. SUBJECT TERMS
ovarian cancer, ID8/ ID8-F3 tumor, PD-1+ dendritic cells, IL-10 blockade, PD-1 blockade, combination therapy, animal models, C57BL/6 mice, intraperitoneal, PD-1 + IL-10, tumor microenvironment, cancer stem cells and DNA vaccine + PD-1 therapy

16. SECURITY CLASSIFICATION OF:			**17. LIMITATION OF ABSTRACT**	**18. NUMBER OF PAGES**	**19a. NAME OF RESPONSIBLE PERSON** USAMRMC
a. REPORT U	**b. ABSTRACT** U	**c. THIS PAGE** U	UU	47	**19b. TELEPHONE NUMBER** *(include area code)* 904-953-6657

Table of Contents

Page

Introduction: Ovarian cancer (OC) is highly immunogenic and generally speaking, higher lymphocytic infiltration is associated with better outcomes. For example, Zhang showed that higher CD3+ T cell infiltration into OC was associated with markedly improved survival [1]. The proposed project will help us understand the cell components of ovarian tumors and their environment, which may prevent currently available therapies from generating an optimal response and may help us to understand why current ovarian cancer therapies sometimes fail. The proposed work will allow us to identify new targets for therapies and improve on existing therapies. Identification of new or improved therapies in an ovarian cancer animal model is a necessary step before these treatments can be tested in a clinical setting. Improved therapies for patients with ovarian cancer will result in reduction of tumors and longer patient survival time. Immune responses generated by the different vaccination strategies targeting tumors are usually suppressed by variety of inhibitory axes that exist in tumors. Recent research suggests that PD-1/B7-H1 axis is the major inhibitory axis in tumor environment including ovarian tumor environment that can blunt the immune responses generated by cancer vaccines. T cells, which are major effector cells that can kill tumors, are known to express PD-1 molecules, and it has been shown that effector functions are impaired by this PD-1/B7-H1 axis [2]. Previously our laboratory has identified a population of ovarian tumor (mouse and human)-associated dendritic cells (which are antigen presenting cells) that express PD-1, and we observed that these cells mediate the suppression of effector T cells [15] .Our laboratory has also recently shown in murine models that PD-1 blockade can suppress and regress tumors in the peritoneal cavity. However, it is possible that, following exposure to checkpoint (e.g., PD-1) blockade, tumors rapidly upregulate compensatory immune suppression mechanisms that prevent their destruction. This hypothesis is the underlying concept developed in the current studies, specifically focusing on PD-1/PD-L1 blockade. Preliminary studies in immunocompetent mouse models of ovarian cancer have provided compelling evidence that alternate immune suppressive pathways are activated during checkpoint blockade with anti-PD-1 including increased levels of regulatory cytokines such as IL-10, up-regulation of PD-L1 on tumor-infiltrating myeloid cells and increased infiltration of immune suppressive cells, in particular, myeloid-derived suppressor cells. Specific objectives of the proposed work include: identification of cellular and immune mediators of resistance to checkpoint (PD-1) blockade, to determine if combination therapy with IL-10 blockade improves T cell immunity and tumor rejection, and to determine if immunization with multi-antigen vaccines prior to PD-1/checkpoint blockade will enhance anti-tumor immunity and improve survival.

PD-1/B7-H1 axis: PD-1 is an inhibitory receptor that is expressed on the surface of many immune cells types such as T cells, B cells, monocytes, NK cells, and dendritic cells. It has two known ligands B7-H1 and B7-DC. Ligation of PD-1 by its ligands derives inhibitory responses that blunt the immune cell responses. In the tumor microenvironment, there is preferential induction of PD-1 as well as B7-H1 on immune cells. Hence upon ligation of this receptor with its ligand B7-H1 a cascade of suppressive pathways emanate downstream of the receptor that inhibit the immune cell responses. This PD-1 receptor ligation to its ligand B7-H1 and the ensuing signaling cascade is termed as PD-1/B7-H1 axis

Progress report

<u>Specific Aim 1</u>. Identify cellular and immune mediators of resistance to checkpoint blockade. The hypothesis states that single agent checkpoint blockade (anti-PD-1) will result in up-regulation of immune suppression, leading to treatment failure. Murine models of OC will be used as a murine equivalent of the human antibodies available to patients.

Aim 1, Experiment 1. **Examine changes in the tumor microenvironment following checkpoint (PD-1) blockade.**

In preliminary studies (unpublished), we have tested the hypothesis that there are potential compensatory mechanisms activated in response to checkpoint blockade. Dendritic cells (DCs), along with macrophages, are the major myeloid-derived constituents of the tumor microenvironment. In our published studies, we have observed that PD-1 was highly expressed on tumor-associated DCs, thus potentially making DCs an important target for PD-1 checkpoint blockade strategies [15]. In this experiment, we have tested the hypothesis that checkpoint blockade results in a compensatory boost in myeloid and lymphoid derived immune suppressive cells which in turn neutralizes the capabilities of the increased anti-tumor adaptive immune cells. Immune cells were purified and will be characterized by flow cytometry and multiplexed cytokine analysis, looking for evidence of increased infiltration immune regulatory cell phenotypes. Control and treated mice will be euthanized for collection of tumors at moribund. Tumors will be investigated for changes in the subsets of infiltrating immune suppressive cells. The weight of the greater omentum was used to measure total tumor burden.

Aim 1, Experiment 1, SUBTASK 1. TO DETERMINE THE AGGRESSIVENESS OF P53 MUTANT CELL LINE AGAINST ITS PARENTAL CELL TYPE

The first aim was to identify a cell line that has more aggressive properties than the conventional ID8 cell lines that is widely used for ovarian cancer models. We received ID8-F3, a p53 knockout model of ID8 cells from the University of Glasgow. After comparing the survival curves of ID8 and ID8-F3 at two different cell numbers, as expected the higher mortality rate was seen in the groups that were injected with more cancer cells as well as the ID8-F3 models have higher aggression than conventional ID8 cells in mice (Fig1).

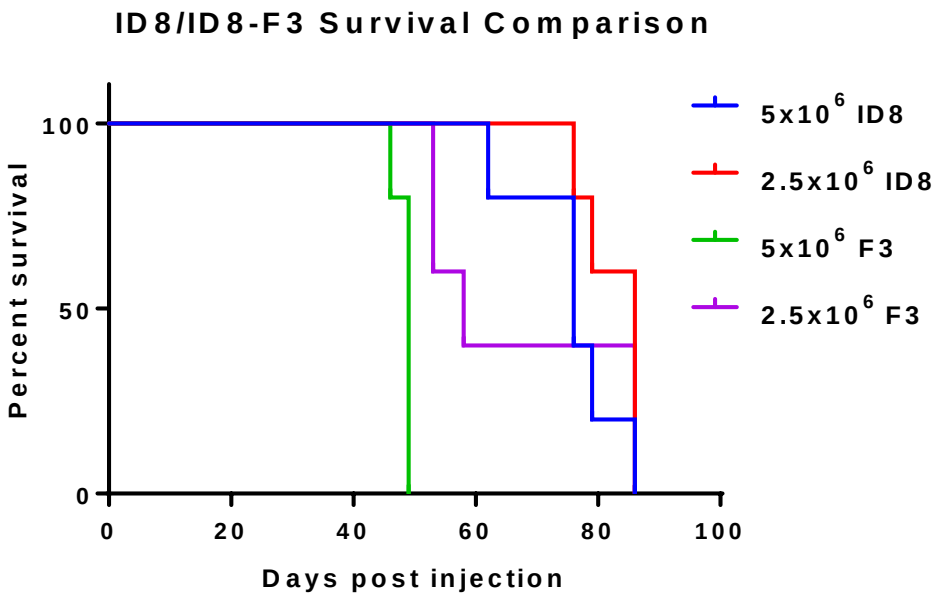

Fig1. ID8/ID8-F3 Survival comparison- The above survival curve indicates the aggressiveness of ID8-F3 over ID8 cells when mice were injected with these cell lines in different cell numbers. In both cases, ID8-F3 has higher morbidity rates than its parental cell line ID8.

Reportable outcomes Aim 1, Experiment 1, Subtask 1: ID8-F3 cell line was more aggressive than conventional ID8 model. Using CRISPR/Cas9 gene editing [3], generated subline of ID8 bearing loss-of-function deletions in Trp53 demonstrated that these alter tumor growth in the peritoneal cavity. However, we believe that a transplantable model, based on a single genetic background (C57BL/6), which recapitulates disseminated peritoneal disease with ascites and in which multiple genotypes can potentially be rapidly investigated in parallel, is an important adjunct to transgenic models.

Aim 1, Experiment 1, Subtask 2.

Flow cytometry panel design

In the present experiment, we designed flow panels to test the hypothesis that checkpoint blockade results in a compensatory boost in myeloid and lymphoid derived immune suppressive cells which in turn neutralize the capabilities of the increase antitumor adaptive immune cells. Despite the presence of anti-tumor immune effectors, however, OCs overcome the immunologic onslaught by complex immune suppression strategies involving infiltration by a variety of specialized lymphoid or myeloid derived suppressor or regulatory cells and/or the direct production and release of factors by the tumor into the tumor microenvironment. Tregs are a heterogeneous T cell subpopulation that produce immune-suppressive soluble mediators (such as TGF-β and IL-10) and use cell contact-dependent mechanisms to halt tumor rejecting immune responses. Myeloid cells appear to constitute the vast majority of OC-infiltrating immune suppressive cells. Dendritic cells (DCs) are in high abundance in OC and they are often immature and immune suppressive. OCs, despite producing danger signals, are

generally ineffective in inducing DC maturation, activation and trafficking to lymph nodes which is thought to be due to tumor-induced alterations in DC differentiation thus reducing the number of functional cells available for effective T cell activation and survival in the tumor microenvironment. Myeloid-derived suppressor cells (MDSCs) and macrophages are also recruited into OC, which blocks local immune activation, and induce tumor-promoting chronic inflammation, often using mechanisms similar to that of DCs [4,5]. Macrophage migration inhibitory factor inhibits the antitumor immune response against OC cells by down regulating NKG2D receptor in NK cells [6]. OCs also express PD-L1 and can directly suppress PD-1+ T cells [7]. Immune cells will be purified and characterized by flow cytometry and multiplexed cytokine analysis, looking for evidence of increased infiltration immune regulatory cell phenotypes including macrophages, MDSCs ($Gr\text{-}1^{lo}CD11b^{+}$ or $Gr\text{-}1^{hi}CD11b^{+}$), immature DCs ($CD11b^{+}CD11c^{+}PD\text{-}1^{+}$), mature DCs ($CD11b{+}CD11c^{+}$Class $II^{hi}PD\text{-}1^{-}$) and Tregs ($CD4^{+}Foxp3^{+}$). We will compare these with effectors such as activated T cells, B cell, and natural killer cells looking at relative proportions. Cell analysis will be done essentially as previously described.

General leukocyte gating strategy

- **For gating CD45+ cells (leukocytes) in every panel**

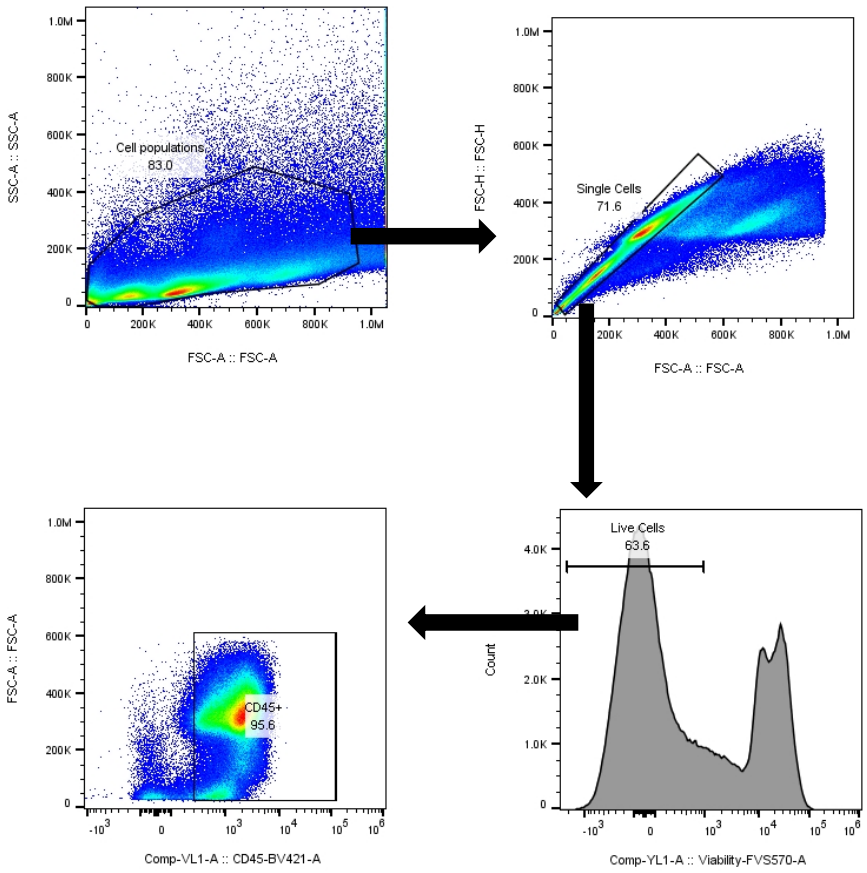

Fig2. General gating strategy- All the flow panels were optimized using naïve spleen cells to understand the baseline of different immune subsets in mice. The above figure describes the scatter of all immune subsets in the spleen which is then gated for single cells from which only live cells are accounted for further analysis. CD45+ cells that are gated are a subset of the live cells. Further analyses were done within CD45+ live cells.

T cell activation gating strategy

- **For gating CD4+, CD8+, γδ T cells and expression of activation marker CD69**

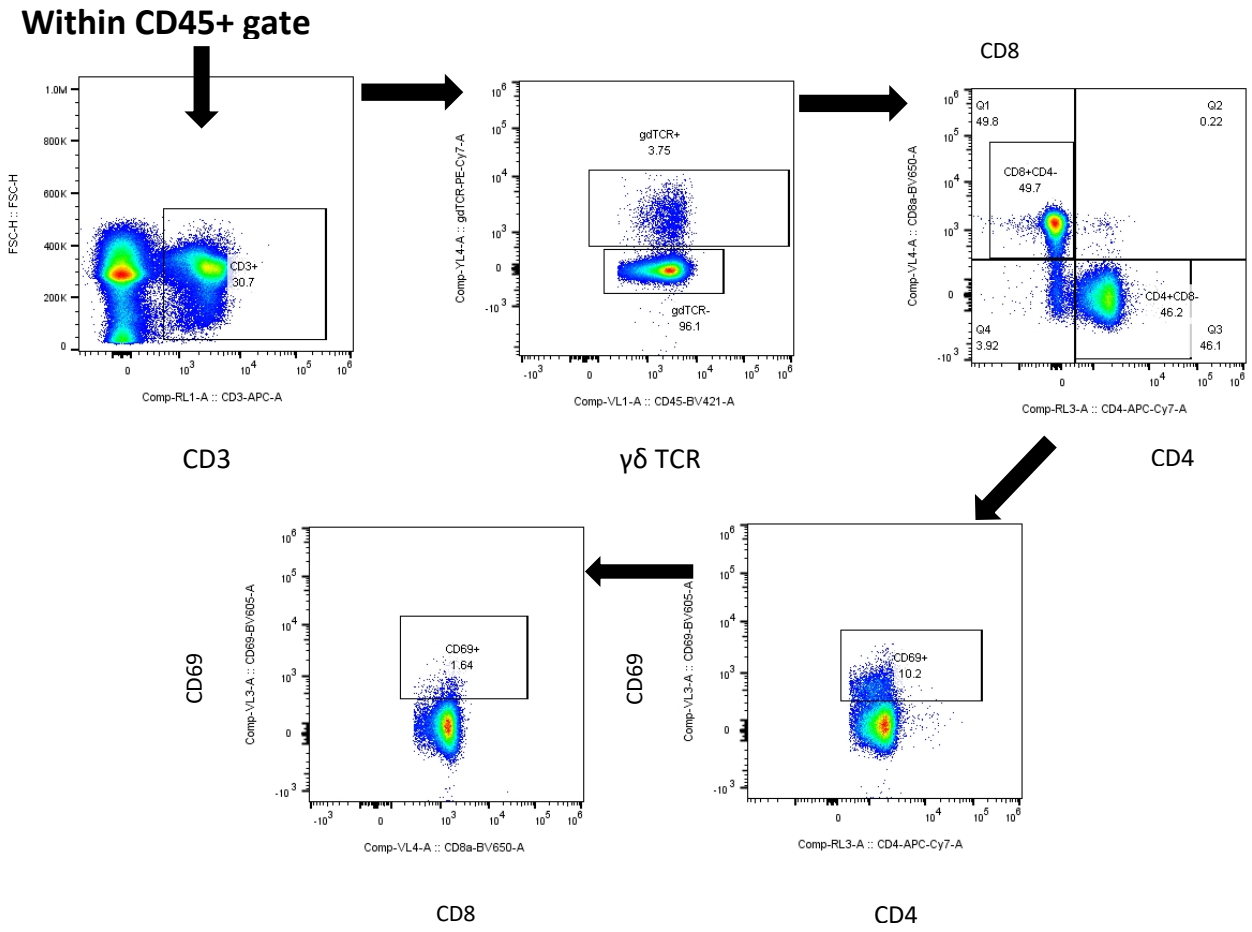

Fig3. T cell activation panel- This figure shows the different T cell subsets within the leukocyte gating (CD45+). T cell receptors which are represented by the CD3 markers are used to identify T cells. Within T cell receptor there are two different subtypes namely αβ- TCR and ɣδ-TCR. More than 80% of the T cells are of αβ subtypes (Fig. not shown). Earlier studies (not shown here) suggested ɣδ-TCR represents immune suppressive phenotype. Moreover the T cells are further classified based on functions namely- T effector (CD8) and T helper (CD4). Both cells were examined for their baseline activation status.

T cell regulation gating strategy

- **For gating T_{reg} cells (CD4+CD25+FoxP3+)**

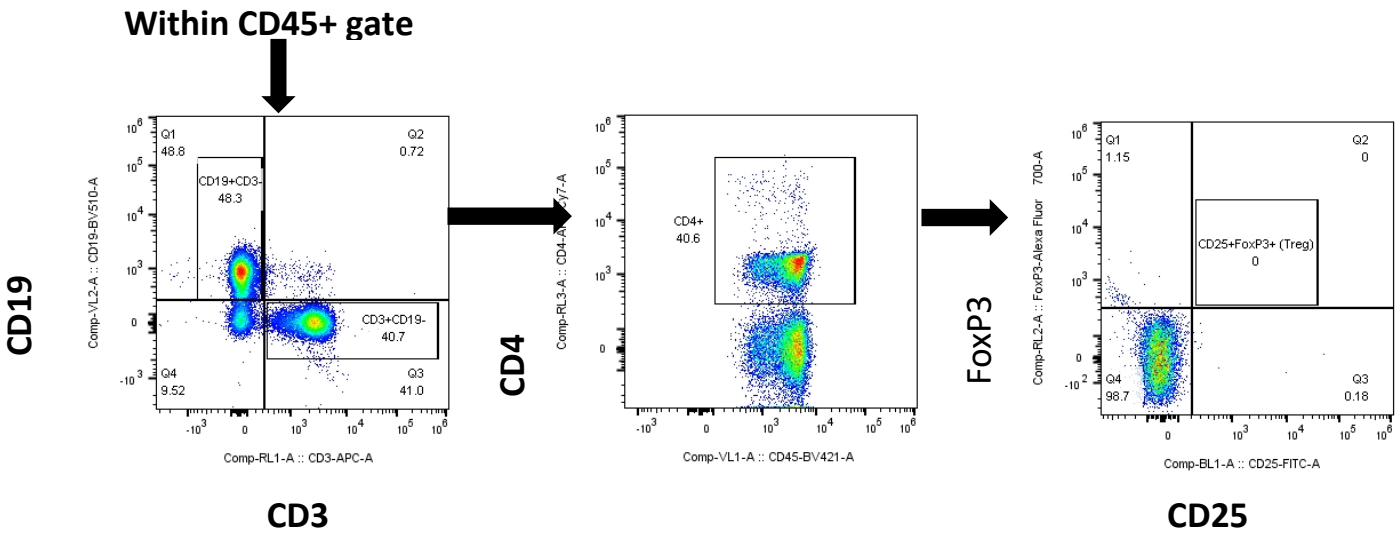

Fig4. T cell regulation panel- This figure represent a subset of CD4 T helper cells also known as T regulatory cells. These are represented by CD4+CD25+FoxP3+ cells. In the above figure there is an undetectable amount of Treg cells. This is because of the fact that Treg cells are <2% of the whole T cell population in naïve mice.

Macrophages/MDSC/NK cell gating strategy

- **For gating Macrophages (F4/80+CD161-), MDSCs (CD11b+Gr-1+CD161+), Natural Killer cells (CD161+F4/80-)**

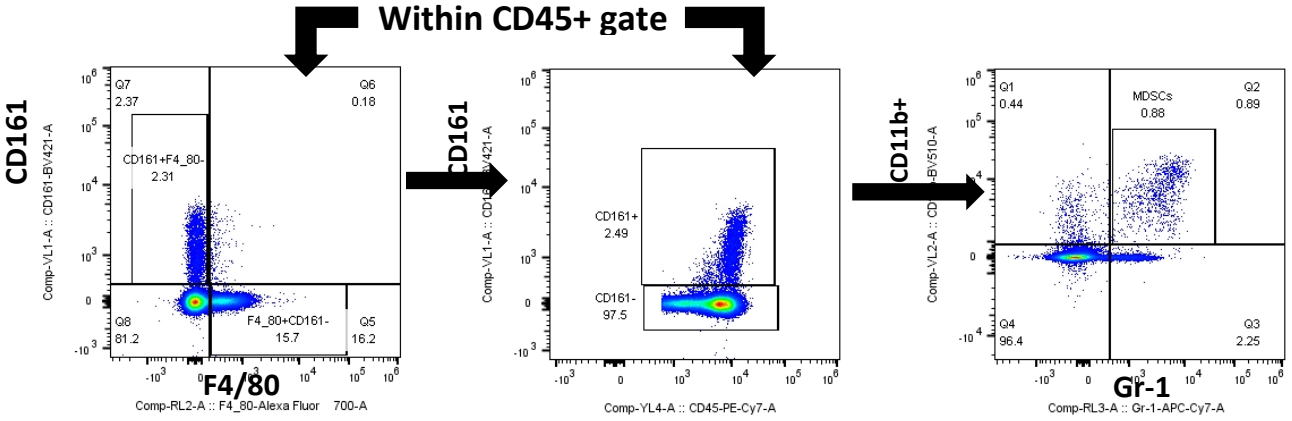

Fig5. Macrophage/ Myeloid derived suppressor cells (MDSCs) panel- This panel represents 3 different immune subsets called macrophages (F4/80+), NK cells (CD161+), MDSCs (GR-1+CD11b+CD161-). Macrophages play a significant part in immunity and immune responses. They assume a defensive role exhibited by their ability to carry on phagocytosis of parasites and microbes. They regulate lymphocyte activation and proliferation and they are essential in the activation process of T- and B-lymphocytes by antigens and allogenic cells. NK cells are cytotoxic cells that play a major role in the host-rejection of both tumors and virally infected cells and are activated in response to interferons or macrophage-derived cytokines. Myeloid-derived suppressor cells (MDSCs) are a heterogeneous population of early myeloid progenitors, immature granulocytes, macrophages, and dendritic cells at different stages of differentiation. These cells are of great interest because they have the capacity to suppress both the cytotoxic activities of natural killer (NK) and NKT cells, and the adaptive immune response mediated by $CD4^+$ and $CD8^+$ T cells.

Dendritic Cell/B cell gating strategy

- **For gating B cells (CD19+CD161-) and dendritic cells (CD11c+CD161-) and expression of PDL1, MHC Class II, and activation markers CD80 and CD86.**

Within CD45+ gate

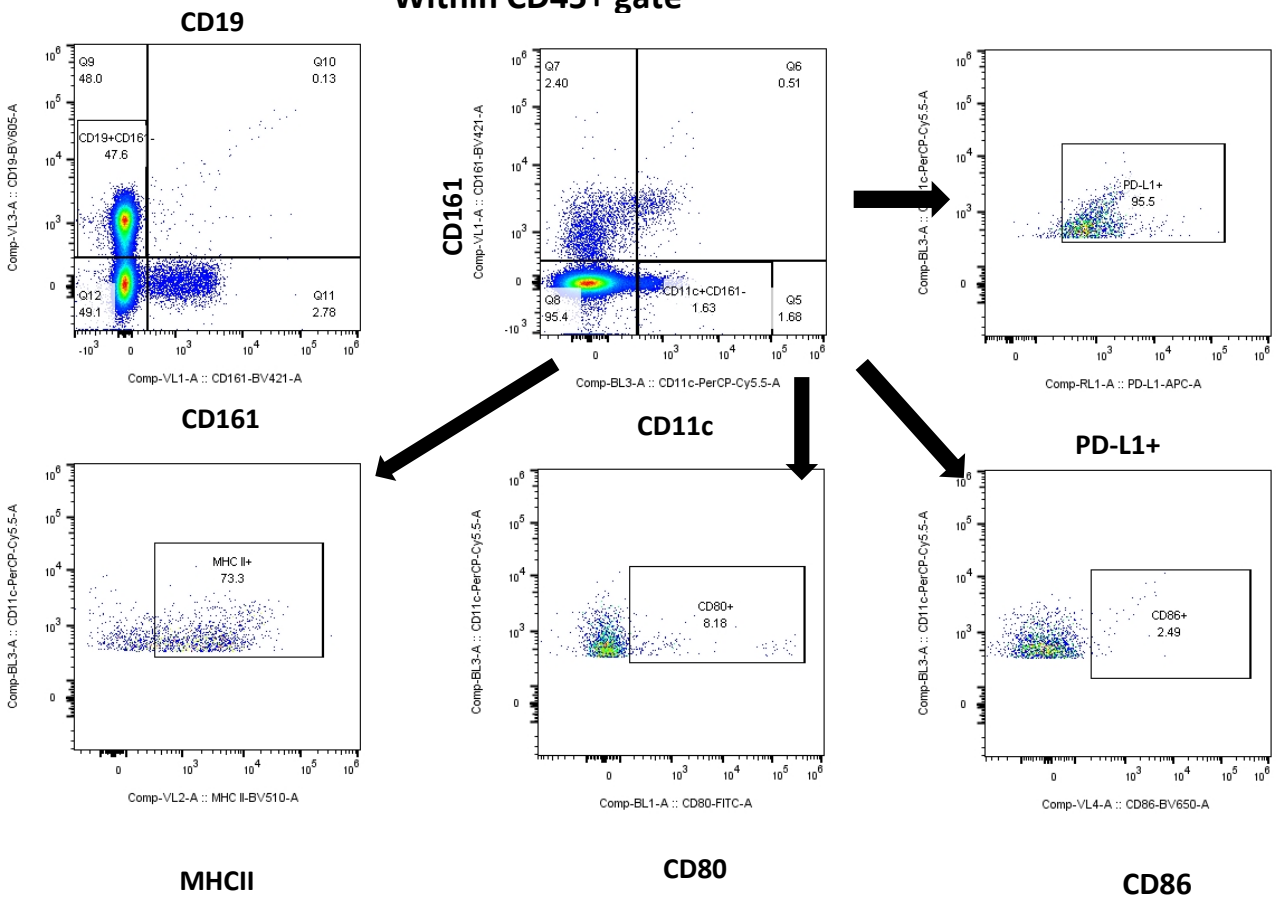

Fig6. DC/ B cell panel- Dendritic cells and B cells are considered as antigen presenting cells (APCs). This panel has multiple co-stimulatory markers that are used to define these two markers. The above figure shows the different co-stimulatory molecules expressed on the surface of DC cells (CD11c+). The B cells (CD19+) have the same con-stimulatory signature (not shown in the above panel).

Reportable outcomes Aim 1, Experiment 1, Subtask 2:. Optimization of panels for different immune subsets has been validated and these panels will be used for further analysis of various experiments proposed in this grant.

Aim 1, Experiment 1, Subtask 3. To assess the survival and tumor burden of mice treated with control and anti- PD1 antibody.

In preliminary studies (unpublished), we have tested the hypothesis that there are potential compensatory mechanisms activated in response to checkpoint blockade. Dendritic cells (DCs), along with macrophages, are the major myeloid-derived constituents of the tumor microenvironment. In our published studies, we observed that PD-1 was highly expressed on tumor-associated DCs, thus potentially making DCs an important target for PD-1 checkpoint blockade strategies [15].

A. Body Weights

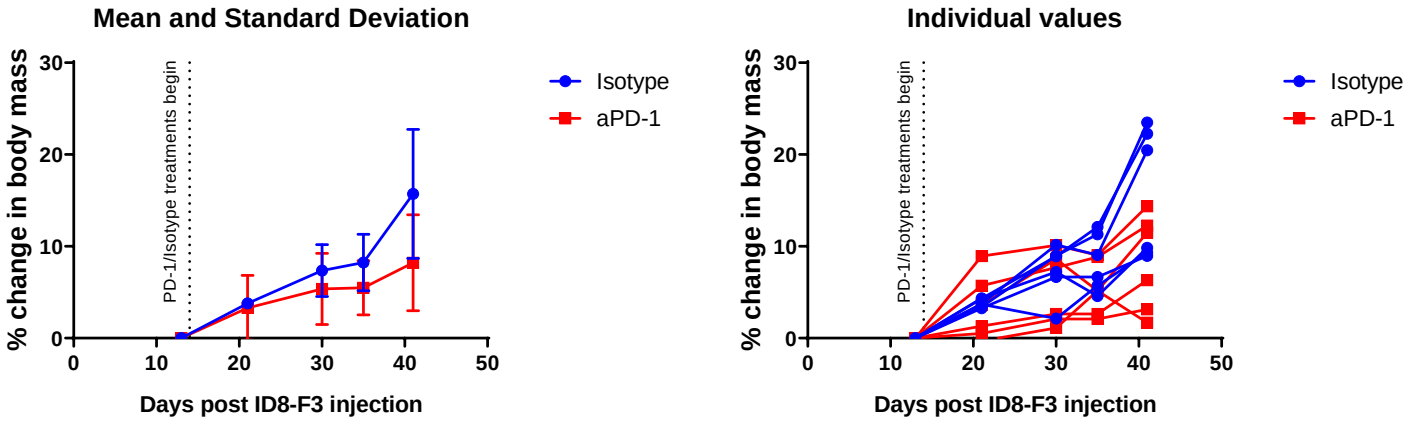

B. Tumor Burden

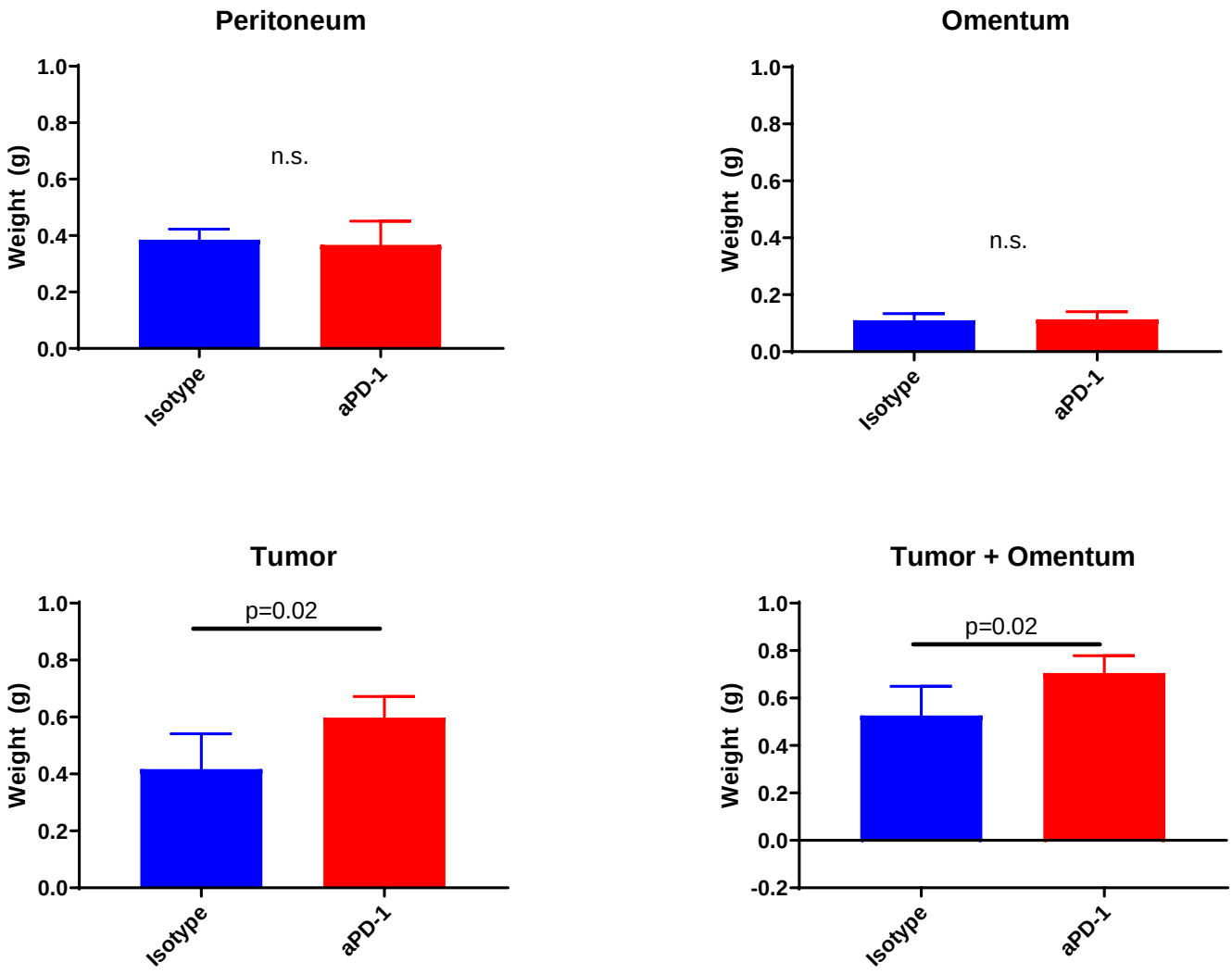

Fig8. Tumor burden and weight assessment. (A) There was no significant change seen in the body mass of tumor bearing mice (n=5) treated with either isotype or anti-PD1 antibody. (B) Both peritoneum and omentum in the treated groups showed no significant change. However, when tumor was measured in the treated mice a significant difference in the anti-PD1 group compared to isotype was observed.

Reportable outcomes Aim 2, Experiment 1, Subtask 3. In this experiment, we have tested the tumor burden in the isotype and anti-PD-1 treated mice. There was a significant difference in tumor weight between the groups in the omentum and not in the peritoneum. This result is in accordance with the previous data published from our lab [8] suggesting that the tumor burden is more in the omentum than the peritoneum.

Aim 1, Experiment 2. Determine whether checkpoint blockade induces immunoediting, resulting in increased tumor resistance to immune eradication.

In addition to immune suppressive cells, the tumor cells themselves may also undergo immunoediting following checkpoint blockade, to acquire an immune suppressive phenotype. Our goal is to test the hypothesis that tumor cells that evade PD-1 blockade have acquired intrinsic resistance pathways. We tested the hypothesis that PD-1 blockade results in a relative increase in the expression of immune suppressive cytokines associated with poor outcomes in ovarian cancer, a phenotype associated with the generation of cancer stem cells (Aim 3), drug and immune resistance in tumor cells (Santisteban et al., 2009; Asiedu et al., 2014; Asiedu et al., 2011).

A Molecules upregulated with aPD-1

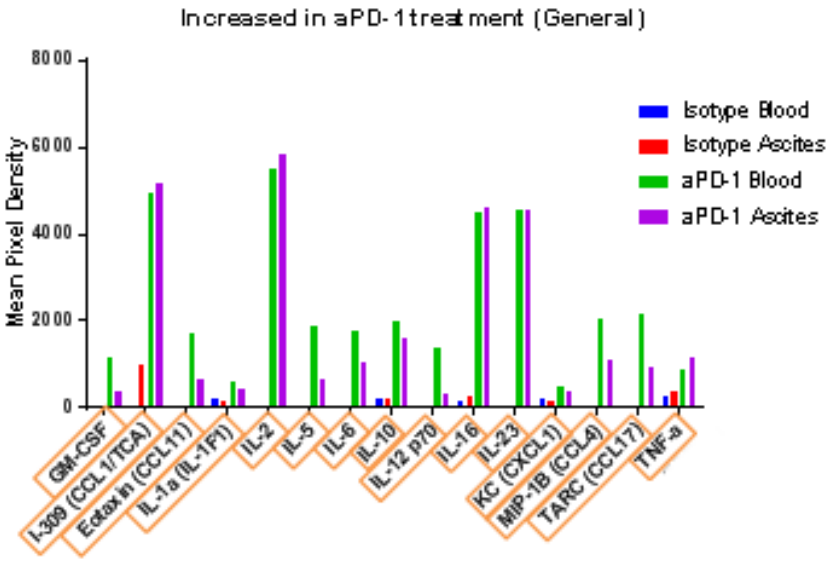

B Molecules upregulated in Ascites

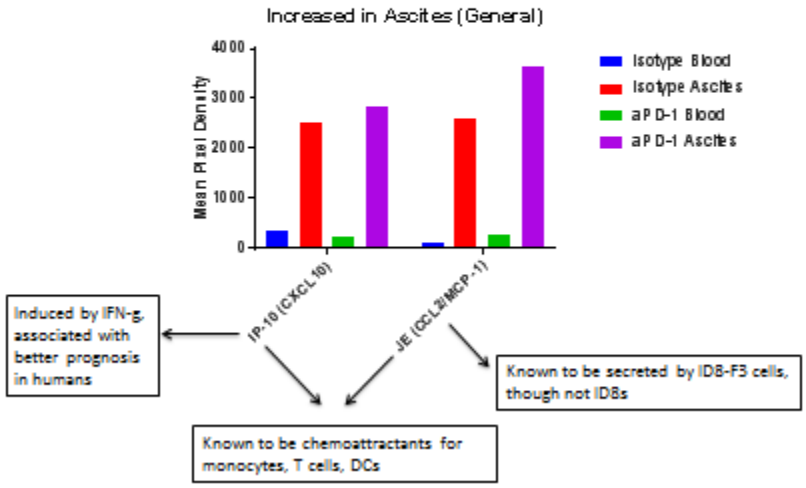

C Molecules upregulated with aPD-1 only in Ascites

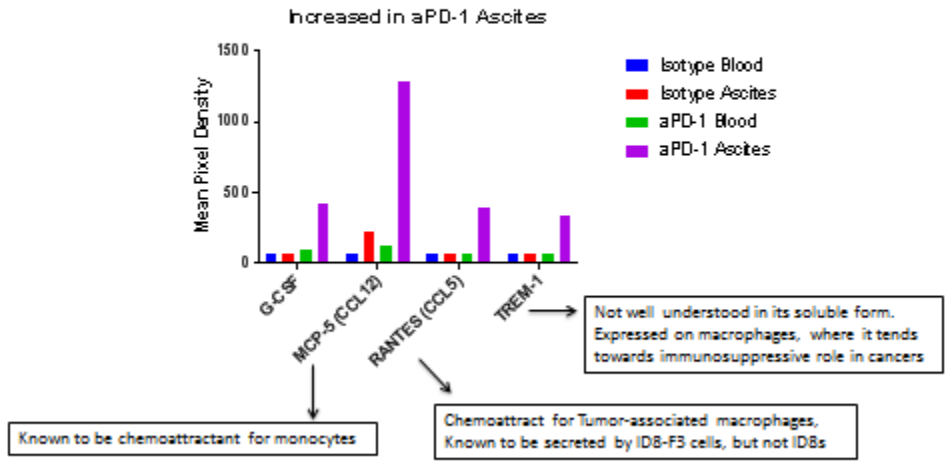

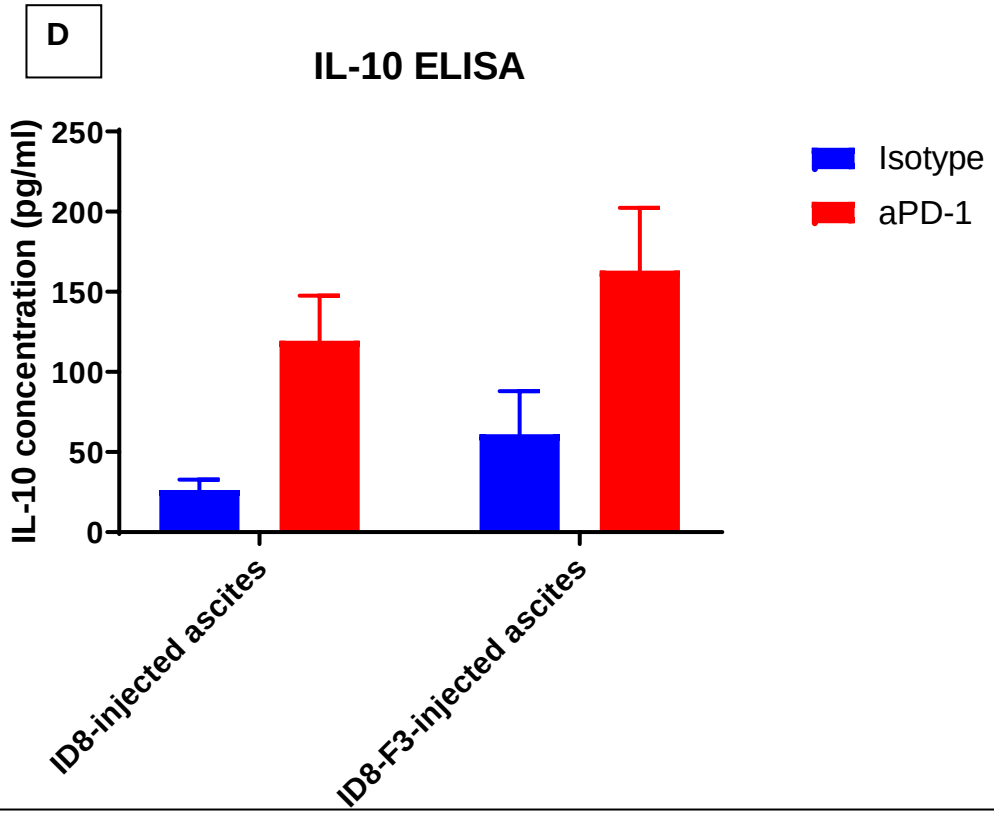

Fig9. Assessment of various cytokines in blood and ascites using cytokine blot array- A) Shows relative increase in different cytokines for control and treated groups in blood and ascites. B) Shows increased cytokine levels in both treatment groups. C) Shows upregulation of cytokines in the anti-PD1 treated group in ascites. **D) Assessment of IL-10 cytokine using ELISA**- Ascites collected from ID8 and ID8-F3 injected mice were processed and DCs were sorted from the ascites using CD11c magnetic beads. These cells were co-cultured with isotype/ anti-PD1 for 24hrs and the media was collected to measure IL-10 response.

Reportable outcomes Aim 1 Experiment 2-. We used cytokine array profiler to test 23 different cytokines to test two treatment groups (from R&D systems). There were increased levels of IL-10 (both in blood and ascites), MCP-5 and CCL-5 (known to be chemoattractant for monocytes) only in the ascites treated with anti-PD-1 antibody (Fig9-A-C). We further investigated the role of IL-10 in both tumor cell lines. In this experiment (Fig9-D), we used both ID8 and ID8-F3 cell lines to test whether our hypothesis of IL-10 upregulation whether it holds for both cell types. We treated tumor bearing mice (n=5) with anti-PD1 and isotype and collected ascites and serum. We sorted Tumor infiltrating dendritic cells from ascites for both treatments and added 200µg of anti-PD-1 to these cells in vitro for 24 hours. The DCs from both cell types significantly upregulated IL-10. Due to the high levels of immune suppressive network that are present in the tumor microenvironment in both models there was no scope of immunoediting that could be observed only with anti-PD-1 therapy. Based on the

findings from above experiments, we further tested the combined effect of anti-PD-1 and anti-IL10 neutralizing antibodies to study the tumor burden.

Aim 1, Experiment 3. **Determine immune regulatory signatures of tumor-infiltrating immune suppressive cells resulting from checkpoint blockade.**

In this experiment, functionality of tumor-infiltrating cells was examined. Above experiment evaluates only the levels of cytokines in tumor microenvironment. However, there may be changes in the functions of the infiltrating cells rendering them more suppressive. For example, we have previously isolated tumor-infiltrating DCs from ovarian tumors, treated them *ex vivo* with anti-PD1 antibody and have evaluated expression of PD-L1, the major mediator of suppression of T cell immunity in the microenvironment. We found that PD-1 blockade results in doubling of the PD-L1 expression which is associated with increased suppressive function [16]. The goal of this experiment was to test the combined effect of anti-PD-1 and anti-IL-10 blockade to evaluate the functional and phenotypic modifications of infiltrating immune suppressive cells leading to augmented immune suppression. Mice were treated 8-11 times, every 3±1 days (2 treatments per week). Control and treated mice were euthanized to harvest tumors on Day 40, 50 and 60 following tumor challenge. Tumor cells were harvested and analyzed for pro- and anti-inflammatory cytokines and/or chemokines, and other regulatory factors. In this study, 6-8 weeks old C57/BL6 mice were injected with ID8F3 cells on Day 0. On day 14, injections with isotype, anti-PD-1, and anti-IL-10/R and in combination were given twice per week for four weeks.

TUMOR WEIGHTS OF DIFFERENT TREATMENT GROUPS

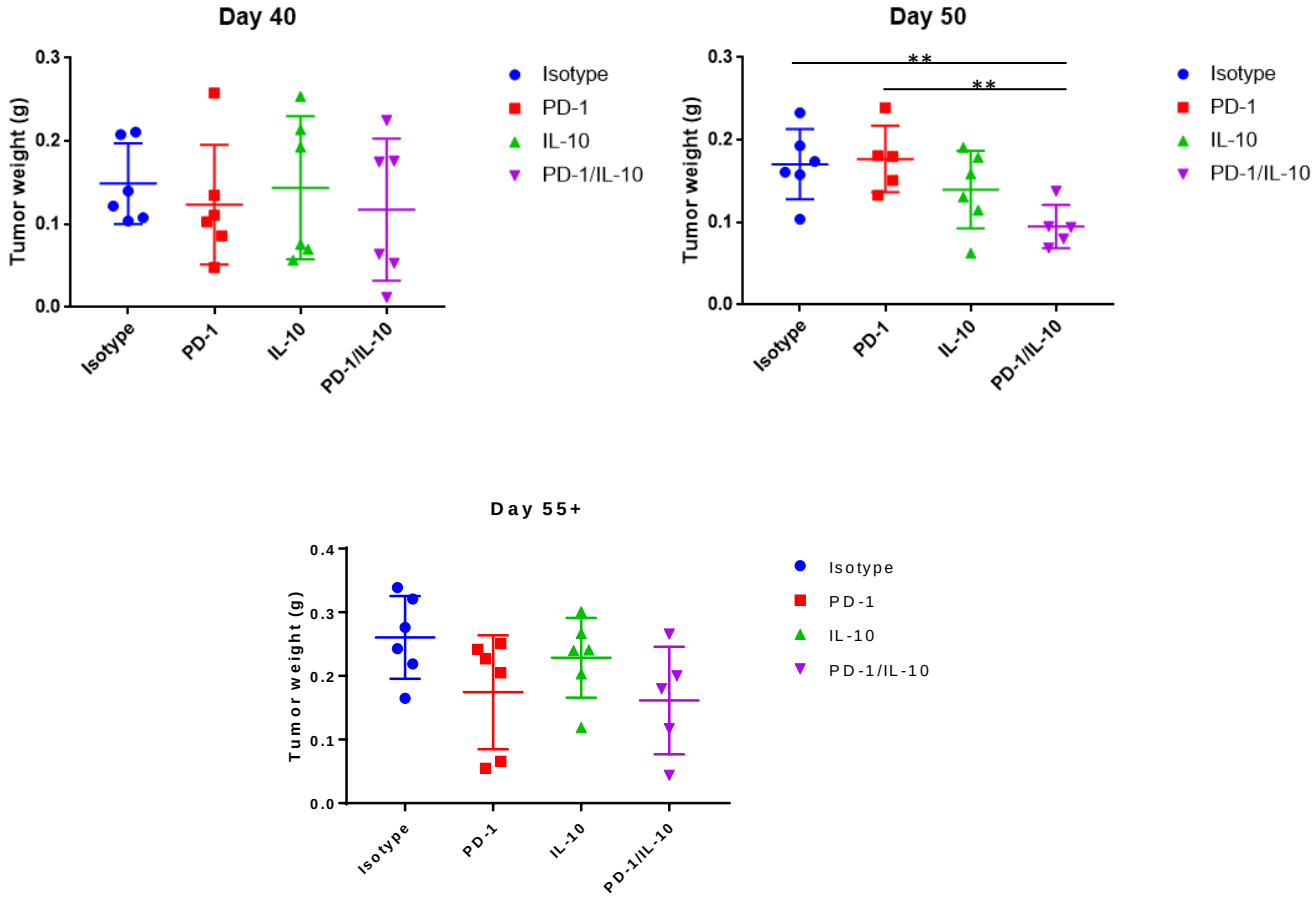

Fig10. Tumors were harvested and weighed on Day 40, 50 and 60 with 6 mice per group. A significant decrease in tumor weights between treatment groups can be observed on Day 50.

IMMUNOPHENOTYPIC ANALYSIS OF DIFFERENT TREATMENT GROUPS

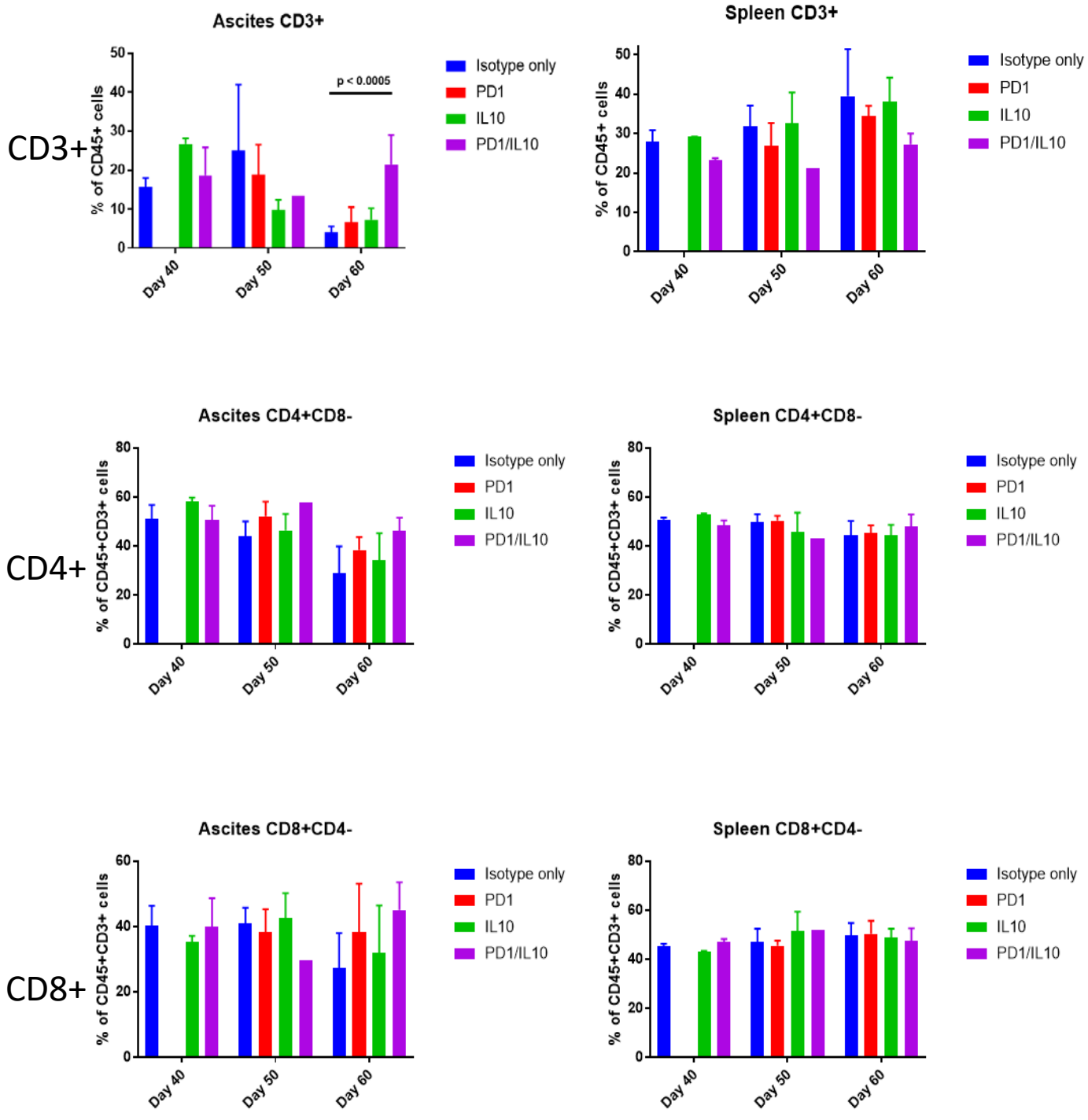

Fig11. Combination treatment leads to a statistically significant increase in the % of T cells (CD3+) on day 60 in ascites. No significant differences were seen between T cell subsets in both spleen and ascites.

Activated CD4+

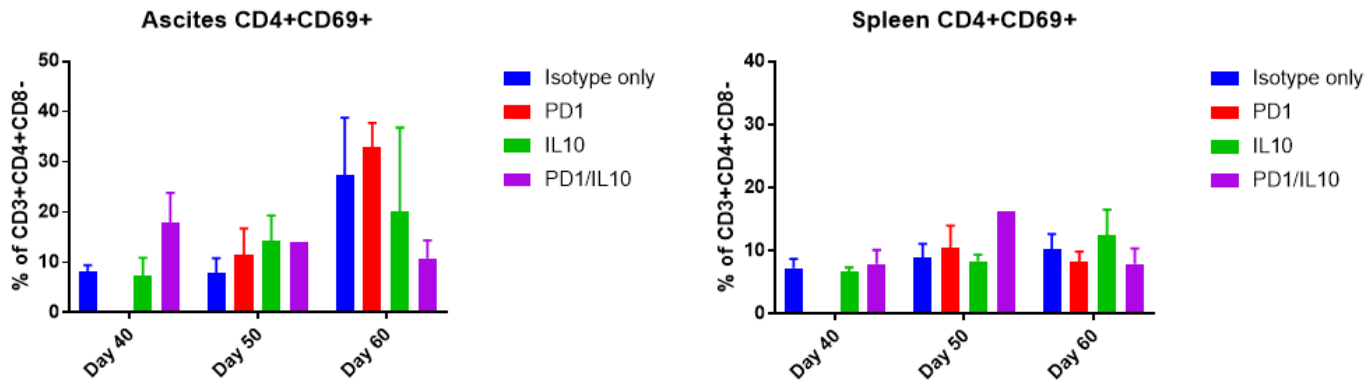

Activated CD8+

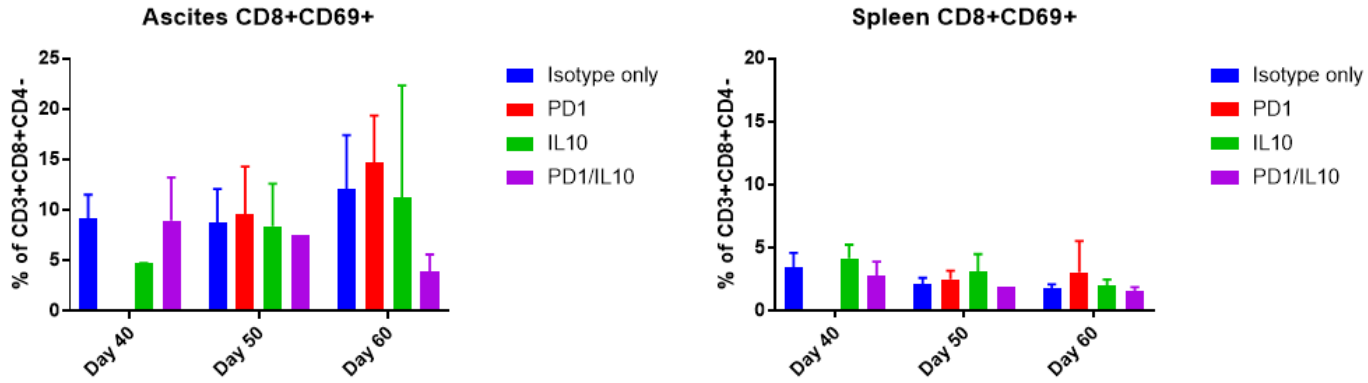

γδ T cells

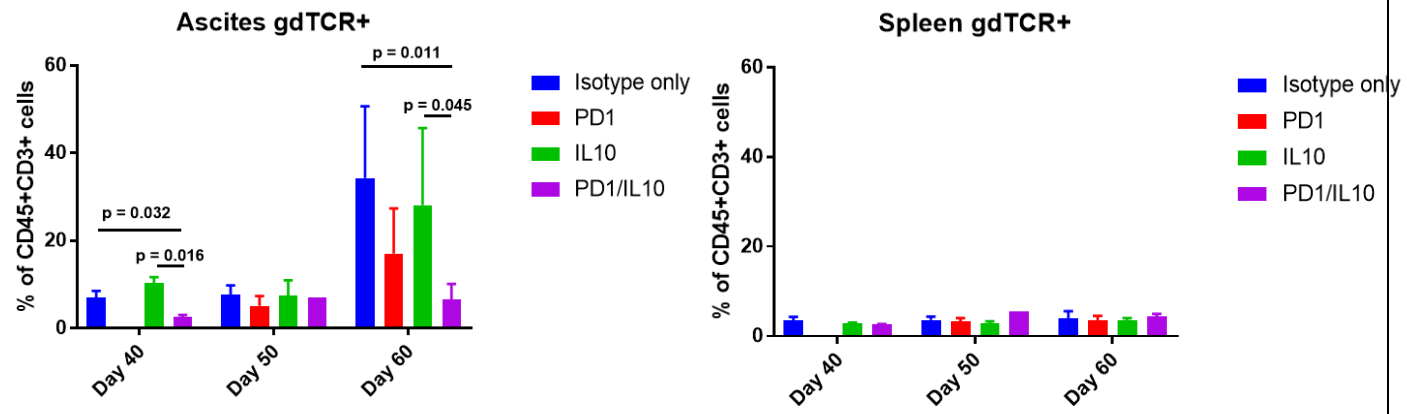

Fig12. Combination treatment leads to a statistically significant decrease in the % of γδ T cells in acites and no significant change was observed in the activation levels of CD4 and CD8 in ascites and spleen

T_{reg}

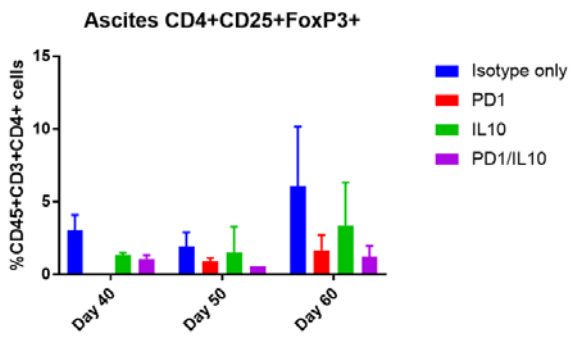

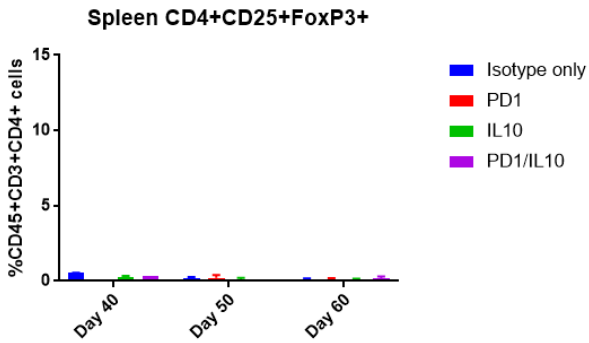

MDSC

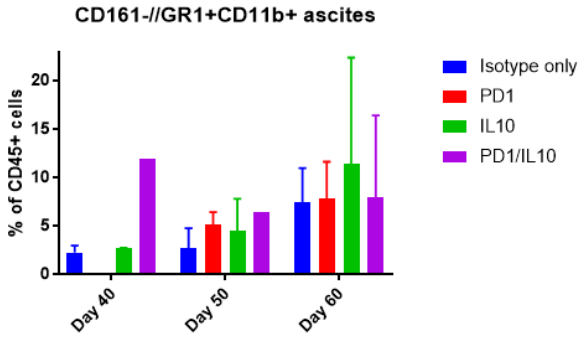

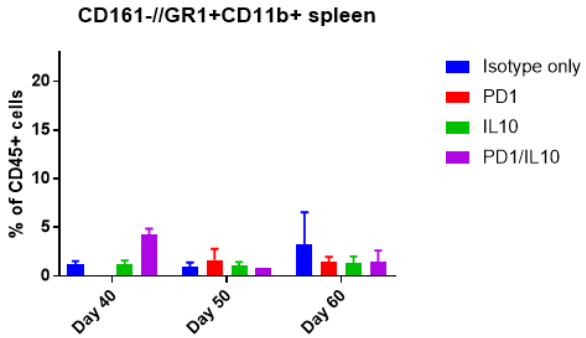

NK cells

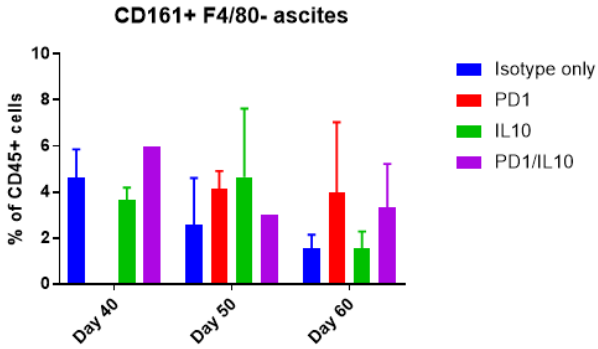

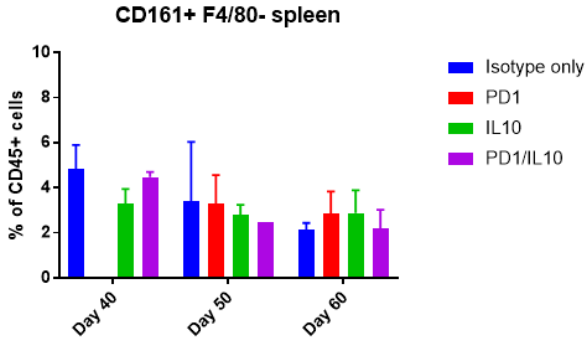

Macrophages

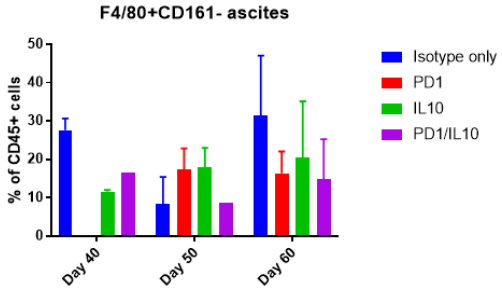

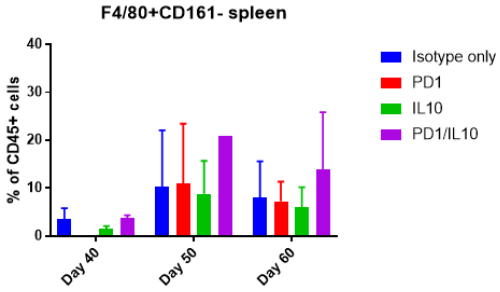

Fig13. No significant changes were observed in the Tregs, MDSCs, NK cells and Macrophages in ascites and spleen.

Dendritic Cells (DCs)

Activated DCs

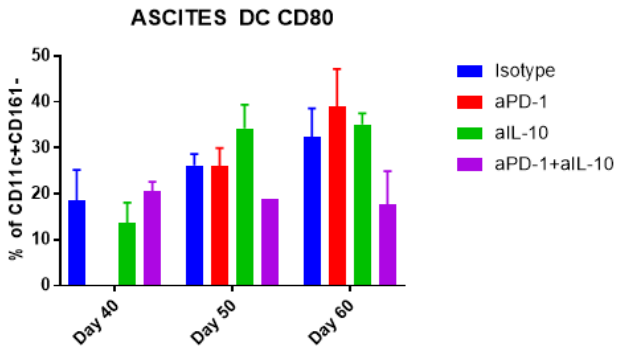

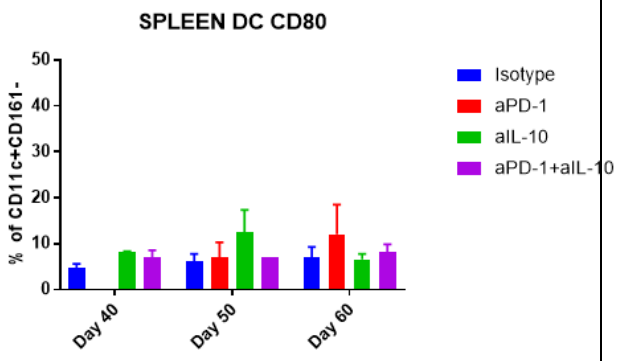

Activated DCs

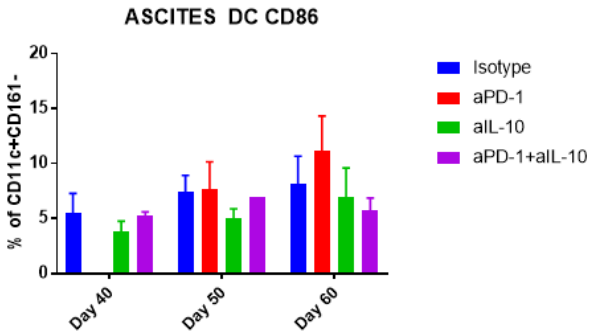

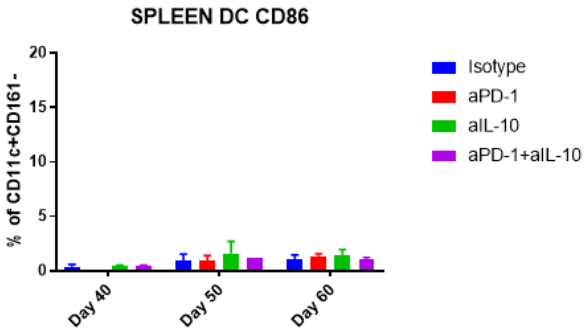

B cells

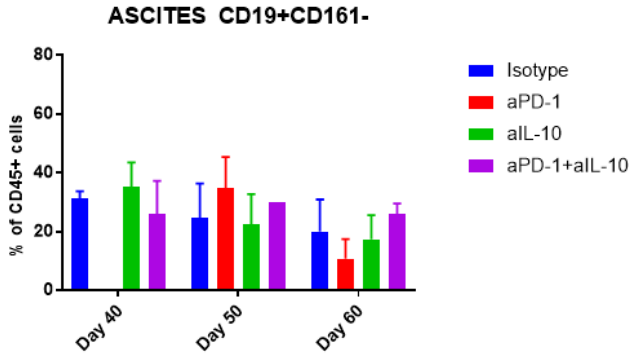

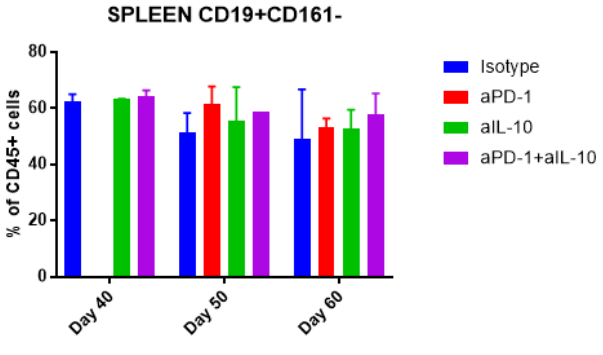

Fig14. No significant changes were observed in the DCs and B cells in ascites and spleen.

Proteome profiler assay to assess the cytokine profile in all treatment groups

A

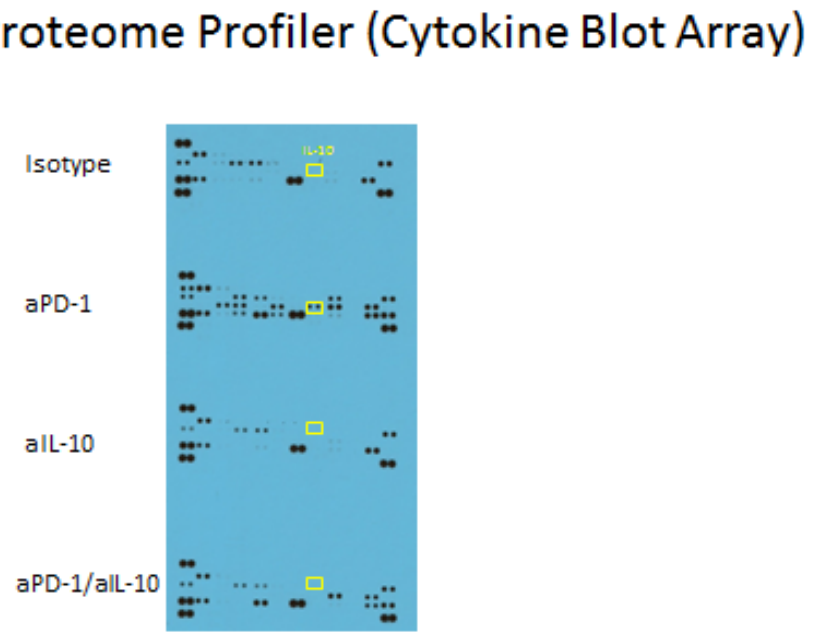

B

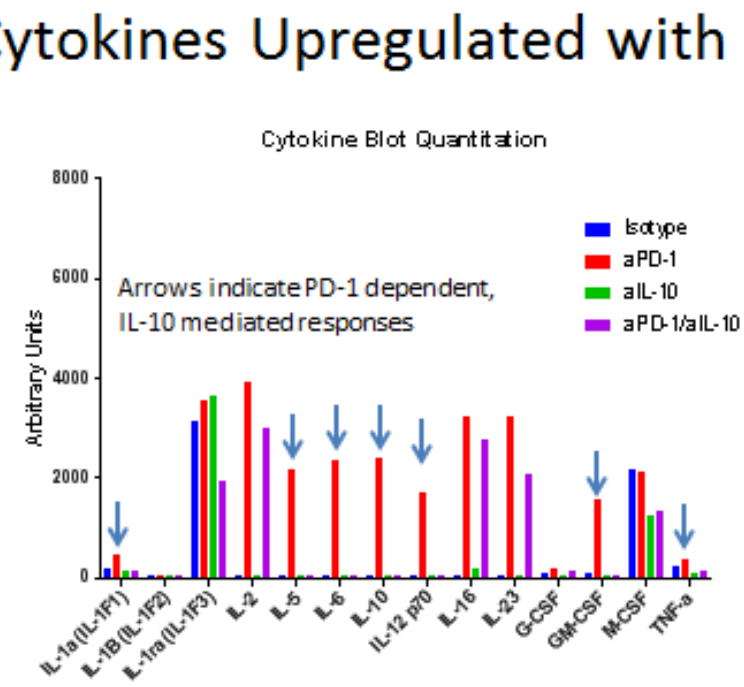

C

Quantitated Analysis of Blot

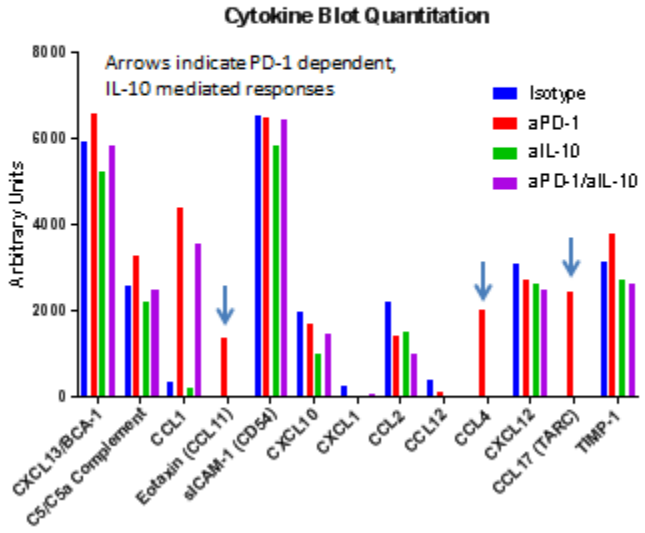

Fig15. (A) Raw data of 23 cytokines expressed in different treatment groups assessed by proteome profiler. Fig (B) and (C) Shows the quantification of cytokine blot for different treatment groups using Image J software. There was an increase in the anti-PD-1 treated group which was not seen in the combined treatment with anti-IL-10.

Reportable outcomes Aim 1, Experiment 3.

We have seen a significant decrease of tumor weight on Day-50 (Fig 10).
In the ascites, there in an increased infiltration of T cells in the combination group compared to the control group (Fig 11). Further, we observed that the γδ-T cells were significantly decreased in the combination treatment (Fig 12). There were no significant changes in the other immune subsets like B cells, DCs, MDSCs, Macrophages, NK cells or Tregs in both ascites and spleen (Fig 13 and Fig 14). We see increased cytokine responses in the anti-PD-1 treated group which is in accordance with the previous experiment (Aim 1, Experiment 2) (Fig15).

<u>Specific Aim 2</u>. To determine if co-blockade of IL-10 synergizes with anti-PD-1 to unmask T cell immunity leading to tumor rejection and improved survival.

The working hypothesis to be tested in this aim is that checkpoint blockade can be combined with other immune therapies for augmented antitumor efficacy. This premise is based on our preliminary data (unpublished) demonstrating that IL-10 is highly upregulated during treatment with PD-1. IL-10 is one of the most potent immune suppressive cytokines. Thus, it is hypothesized that co-blockade of compensatory immune suppressive networks during treatment with anti-PD-1 may lead to synergistic tumor rejection and possibly long term durable remission.

Aim 2, Experiment 1. To determine the duration of the anti-tumor efficacy of combination PD-1 and IL-10 blockade as well as the potential for durable remissions.

We will use the ID8 model (Krempski et al., 2011) in the pilot to evaluate (1) the median improvement in survival in terms of time (weeks or month), (2) tumor burden, and (3) whether tumors that grow out despite demonstrate evidence of immunoediting or if other suppressive networks are activated. Once the tumors are established, mice will be treated intraperitoneally with respective antibodies at intervals of 3-5 days.

Aim 2, Experiment 1, Subtask 1. **Combination treatment enhances survival of tumor bearing mice**

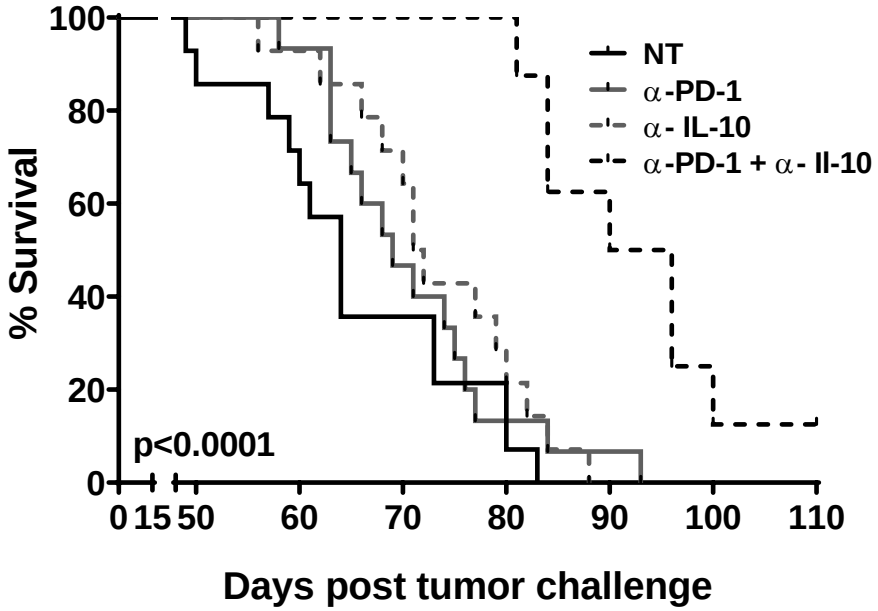

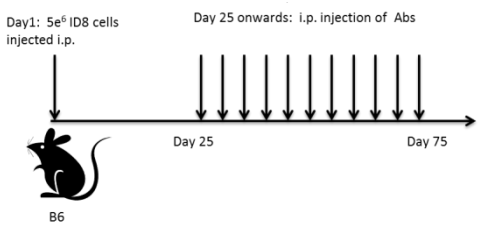

Fig16. Combination of PD-1 blockade and IL-10 neutralization reduces tumor burden and enhances survival of tumor bearing mice- shows Kaplan-Meier plot of ID8 tumor-bearing mice (N=12–16) that were treated intraperitoneally with respective antibodies starting at day 25 post tumor implantation.

Reportable outcomes Aim 2, Experiment1, Subtask1- In the present work, we have identified the TME-associated cytokine IL10 as a critical regulator of the PD-1–PD-L1 axis in the TME. First, we found that IL10, a cytokine whose expression in increased in the TME of several cancers, is capable of increasing PD-1 surface expression in a STAT-3–dependent manner (data not shown). Second, we found that blockade of PD-1, with an antagonistic monoclonal antibody, on DCs led to increased release of IL10 by DC (data shown in Aim 1). Here we show that PD-1 blockade and IL10 signal antagonism as a combination therapy, using blocking antibodies, enhances the antitumor effect in ovarian cancer-bearing mice, leading to significantly improved survival and decrease in tumor burden.

Aim 2, Experiment 1, Subtask 2. **Combination treatment reduces the tumor burden**

Endpoint determined based on the abdominal distension/ascites volume

Tumor weight = (Tumor disseminated omentum - Age matched healthy omentum)

Tumor measurements at end point

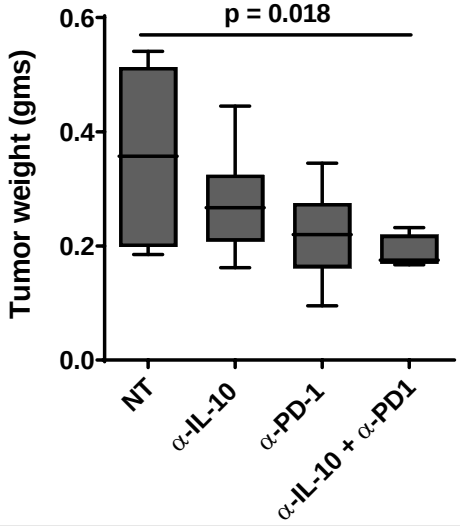

Fig17. Combination of PD-1 blockade and IL-10 neutralization reduces tumor burden and enhances survival of tumor bearing mice. Mean tumor weights in grams (+/- SEM, N=5-6), from different treatment groups, as measured at the time of ascites harvest.

Reportable outcomes Experiment1, Subtask2- IL10 has a major role in evasion of immune-mediated regression of tumor following checkpoint blockade in the present model which is demonstrated by the observation that combination treatment, blockade of PD-1 and IL10(R) significantly reduce the tumor burden.

Aim 2, Experiment 1, Subtask 3: Demonstrating evidence of immunoediting and activation of other suppressive networks

A

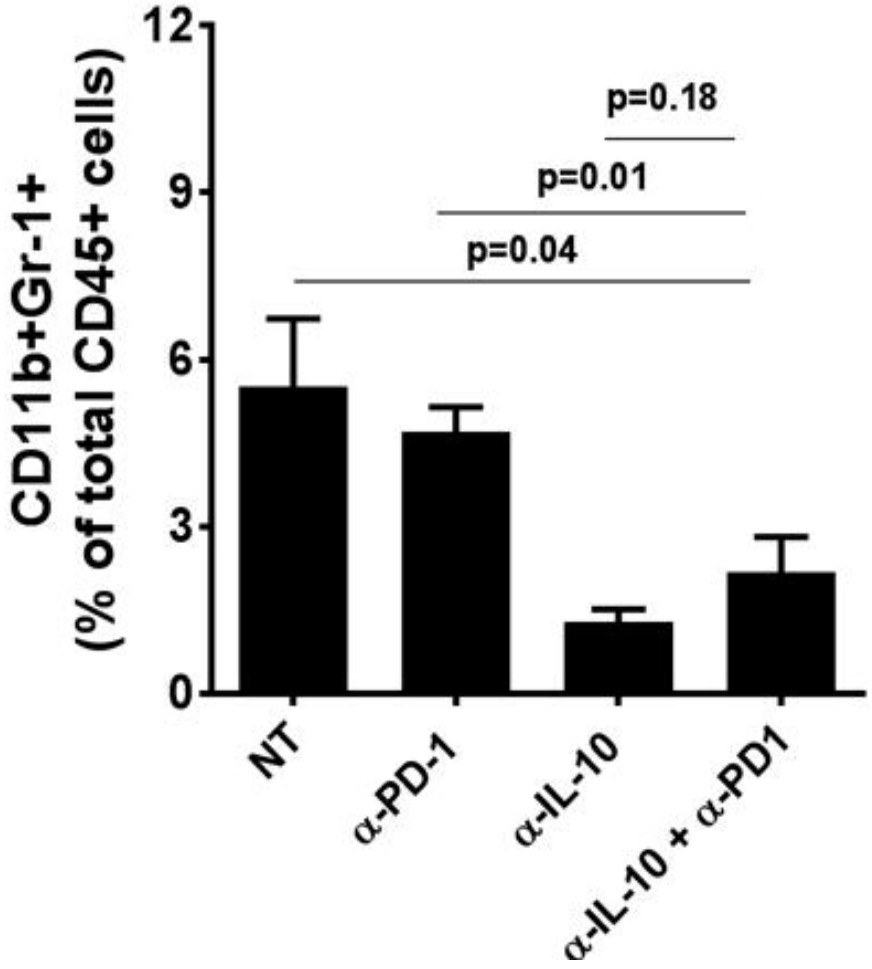

Fig18. A) Combination treatment results in decreased infiltration of MDSCs in the ascites of tumor bearing mice

Panel A shows the MDSC population represented by $CD11b^{+}Gr1^{+}$ cells in the ascites from different treatment groups. For analysis, live cells were pre-gated on $CD45^{+}$ cells, the mean frequency (±SEM, N=5–7) of $CD11b^{+}Gr1^{+}$ cells in the ascites of the different treatment groups.

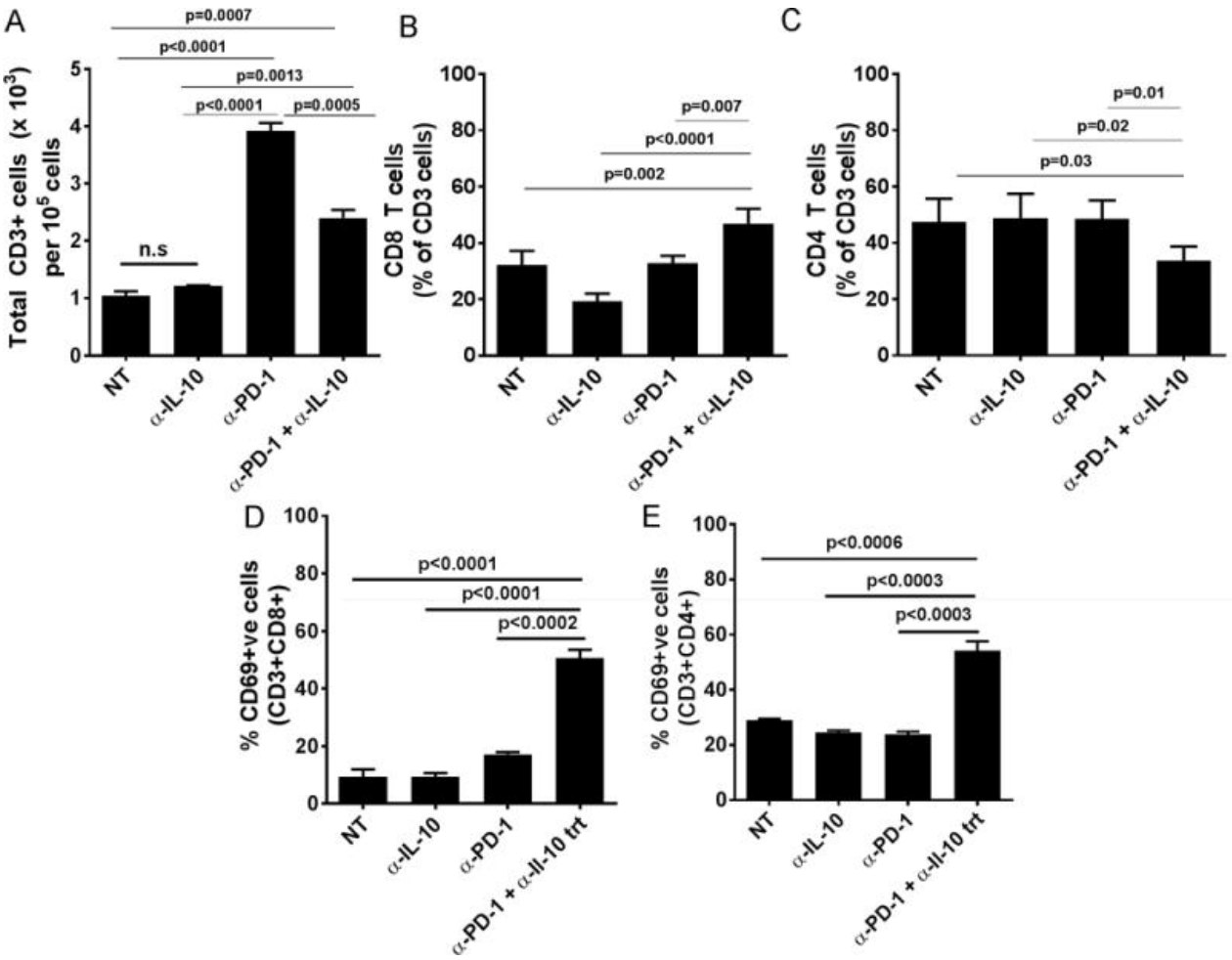

Fig19. Combination treatment enhances the infiltration of activated T cells in the ascites of tumor bearing mice

Panel A shows are the mean (±SEM, N=6) number of T cells per 1 × 105 leukocytes in the ascites of tumor-bearing mice from different treatment groups. **Panels B–C** show the mean (±SEM, N=4) percentages of CD8+ T cells (Panel B) and CD4+ T cells (Panel C) among total CD3 cells from the ascites of tumor bearing mice from treatment groups. **Panels D–E** show the mean (±SEM, N=5–7) percentages of CD69+ cells among CD8+ T cells (Panel D) and CD4+ T cells (Panel E) from the ascites of tumor bearing mice from treatment groups.

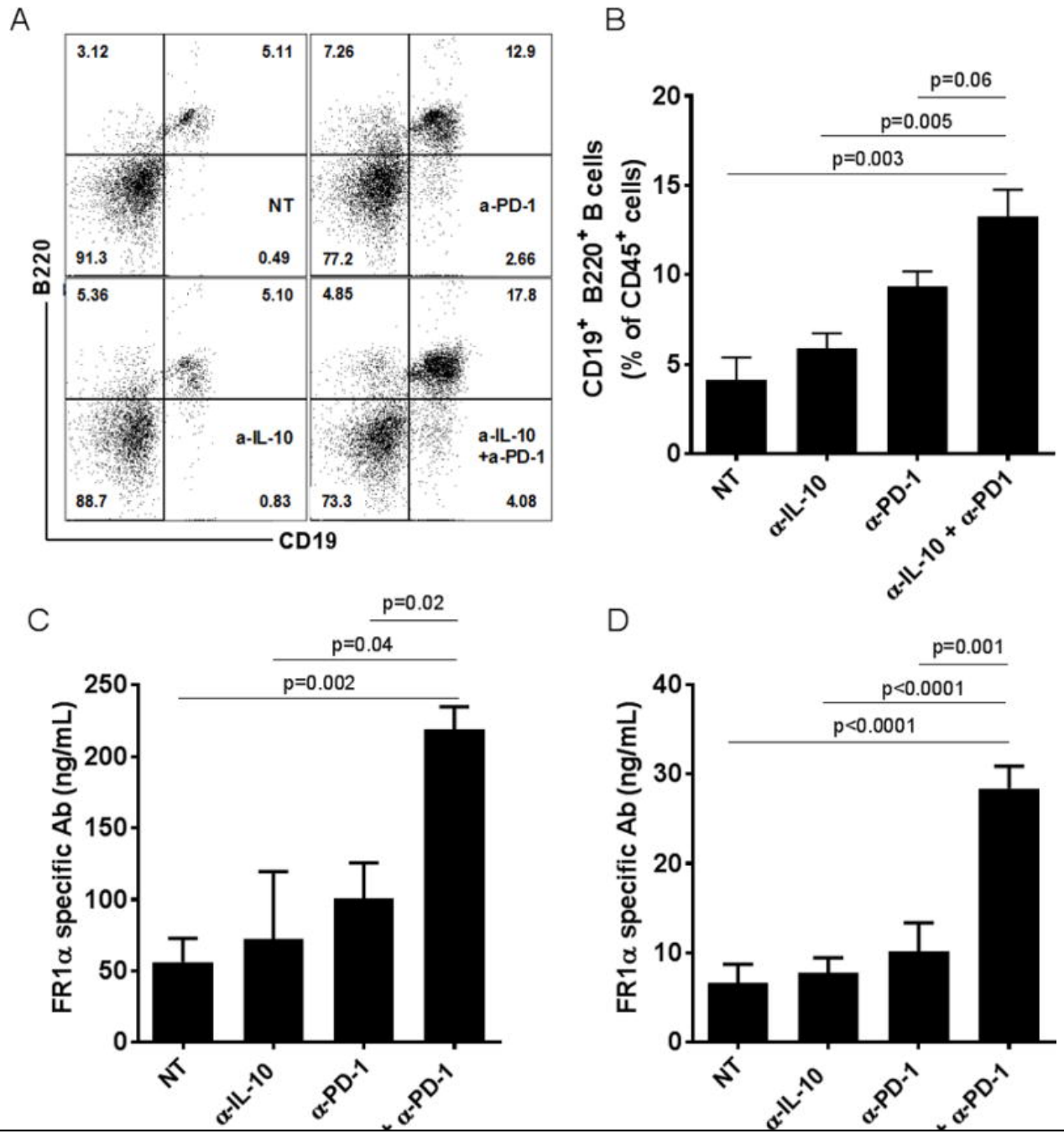

Fig20. Combination treatment enhances the antigen specific antibody response in tumor bearing mice

Panel A shows the representative dot plot and **Panel B** shows a bar graph of the mean frequency (±SEM., N=4–5 replicates) of CD19+B220+ B cells among CD45+ cells from the ascites of tumor-bearing mice. **Panels C and D** show are the mean levels (ng/ml) of FRα specific antibodies measured in the serum (±SEM, N=3 replicates) and ascites (±SEM, N=7 replicates) respectively, of mice from the different treatment groups.

Reportable outcomes Aim 2, Experiment 1, Subtask 3- We observed decrease in MDSCs represented by Gr-1+CD11b+ cells (Fig18). This indicated the combination treatment has enhanced the efficiency by decreasing the suppressive networks in tumor microenviroment. As a result, there is an increase in activated T cell population in the ascites (Fig19). Moreover, production of antibodies against FR-alpha, an antigen present on ID8 tumor cells is an indication of immunoediting in this tumor model. (Fig20).

Aim 2, Experiment 2. To identify the mechanistic underpinnings of the therapeutic efficacy of combination PD-1 and IL-10 Blockade.

In particular, this experiment will investigate the role of T cells in tumor rejection. We examined the tumor/ascites-infiltrating T cells from treatment groups in Experiment 1. To determine a role for T cells in this model, we depleted CD8 or CD4 T cells beginning at the time of PD-1 therapy with antibodies as we have previously published (Karyampudi et al., 2015). CD4 and CD8 blocking antibodies were obtained from the core facility.

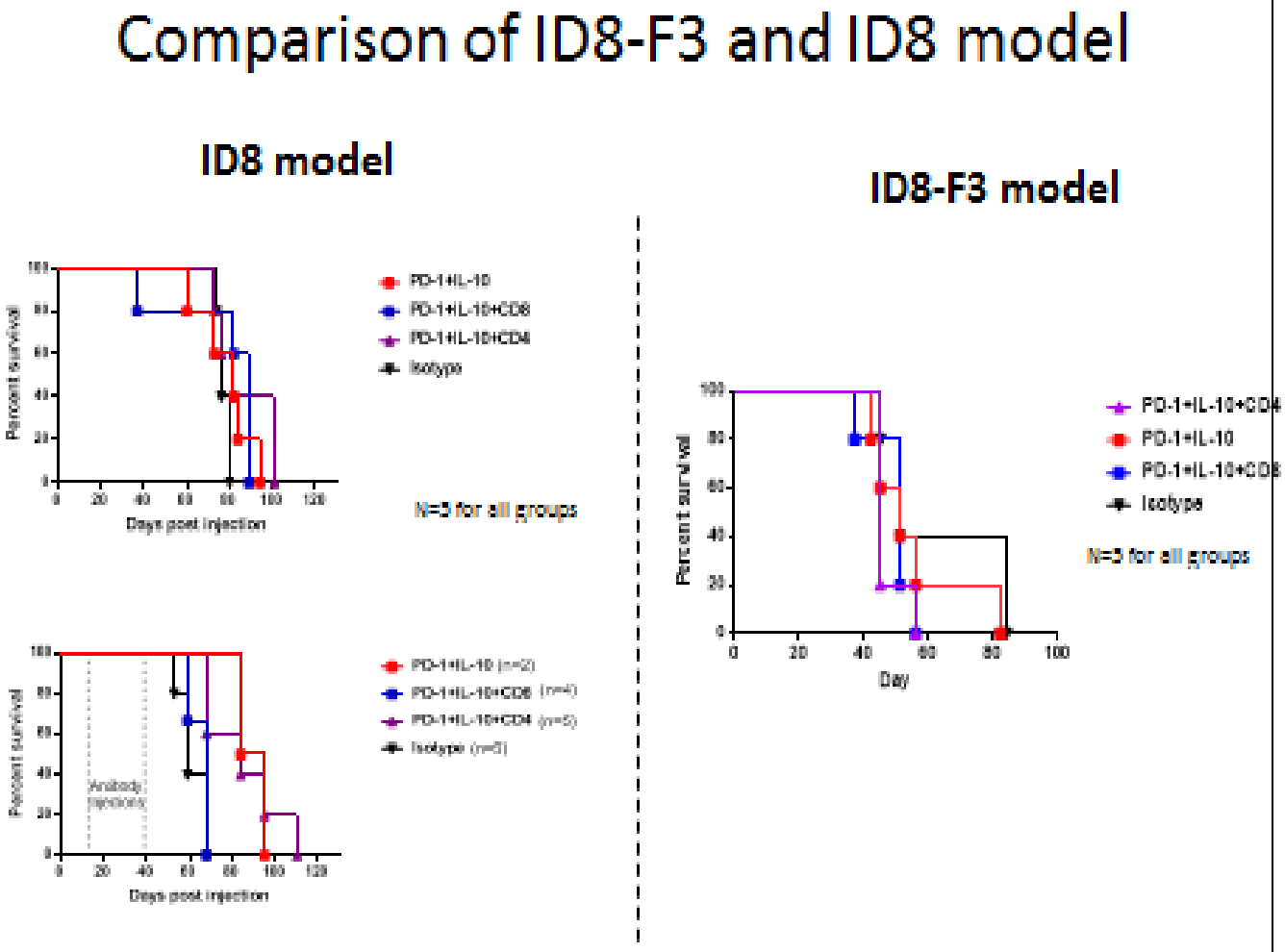

Fig21. Efficacy of T cells in ID8 and ID8-F3 models were demonstrated using neutralizing anti-CD4 and anti-CD8 antibodies. Anti-CD8 T cells are the key to survival of tumor bearing mice in ID8 model whereas the effect of both anti-CD4 and anti-CD8 is seen in ID8-F3 tumor bearing mice when used in combination with anti-IL-10 and anti-PD-1.

Reportable outcomes Experiment2, Subtask2- In the ID8 model, mice that received the anti-CD8 antibody in combination with anti-PD-1 and anti-IL-10 showed poor prognosis indicating the effect of CD8+ T cells is important for survival .However we did not see the same effect with anti-CD4 in this model. On the contrary, we saw the effect of both anti-CD4 and anti-CD8 T cells is more pronounced in the ID8-F3 model as the mice treated with neutralizing T cell antibodies had much lower survival rate compared to the effect of anti-PD-1 and anti-IL-10 alone. Even though we can see a clear difference on the effect of T cells in this model, it is important that we need to add more arms treating the tumor bearing mice only with neutralizing T cell antibodies alone to clearly explain the importance of T cells in the tumor microenvironment. However, based on the survival curve, we clearly see that these two models do not have the same tumor microenvironment even though the ID8-F3 was derived from the parental ID8 cell line.

<u>Specific Aim 3</u>: To determine if pre-immunization with antigen-specific vaccines augments anti-PD-1 efficacy.

PD-1/PD-L1 based blockade therapies inhibit key regulatory loops in the tumor microenvironment leading to clonal expansion of antigen-specific anti-tumor T cells. Tumor eradication is slower than standard chemotherapeutics because T cell immunity activated in response to checkpoint blockade requires clonal expansion, which typically takes weeks to achieve, allowing the tumors sufficient time to evade the immune response. Preliminary data suggests that multi-antigen vaccines targeting malignant epithelial tumor cells, ovarian cancer stem cells, and tumor-associated stroma effectively augment clonal expansion of tumor antigen-specific T cells leading to more complete and durable responses to checkpoint blockade. We proposed that vaccination prior to checkpoint blockade will elevate the levels of anti-tumor T cells to threshold levels required so that clonal expansion outpaces development of compensatory immune suppression, leading to durable regression.

Aim 3, Experiment 1. Determine whether multi-antigen epithelial and stem cell targeting vaccines block ovarian cancer growth.

Cancer stem cells (CSCs) have been identified in ovarian cancer tumors, and they are resistant to conventional cancer treatments. Subsequent studies have identified CSCs in solid tumors including OC [9-14]. The current aim was to identify stem cell markers and subsequently select a panel of overexpressed self-antigens which are common in murine and human cell lines.

Aim 3, Experiment 1, Subtask 1. **Enrich stem cell populations by sphere forming assay to sort for CSCs marker**

The tumor spheres express high levels of SC markers and exhibit a great degree of tumorigenicity. Using sphere assays for tumor cells, a number of groups have demonstrated that CSCs efficiently form tumor spheres in a clonogenic manner [17]. These tumor spheres are also chemoresistant and exhibit the upregulation of drug-resistance proteins [15].

For this aim, we investigated 4 cell lines (2 mouse, 2 humans) to characterize cancer stem cell markers and sphere formation. We used ID8 and ID8-F3 cell lines as the murine models and A2780 and SKOV3 as the human counter parts.

A

SKOV3

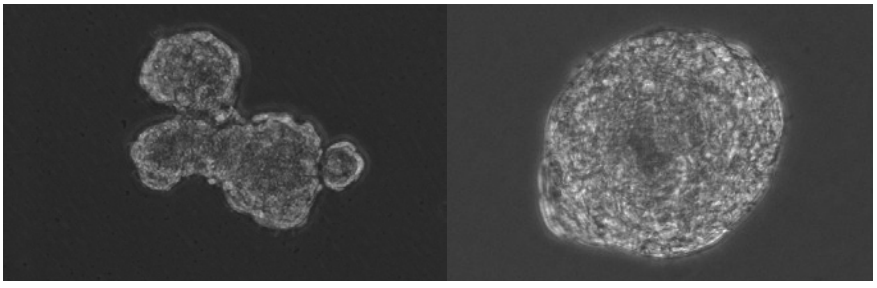

4 day culture (10x) 7 day culture (10x)

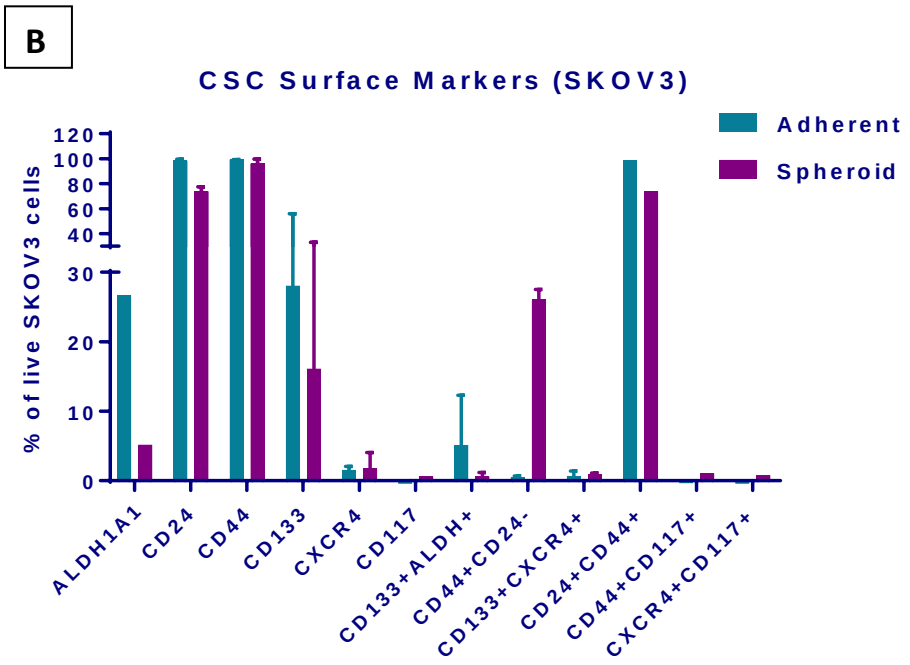

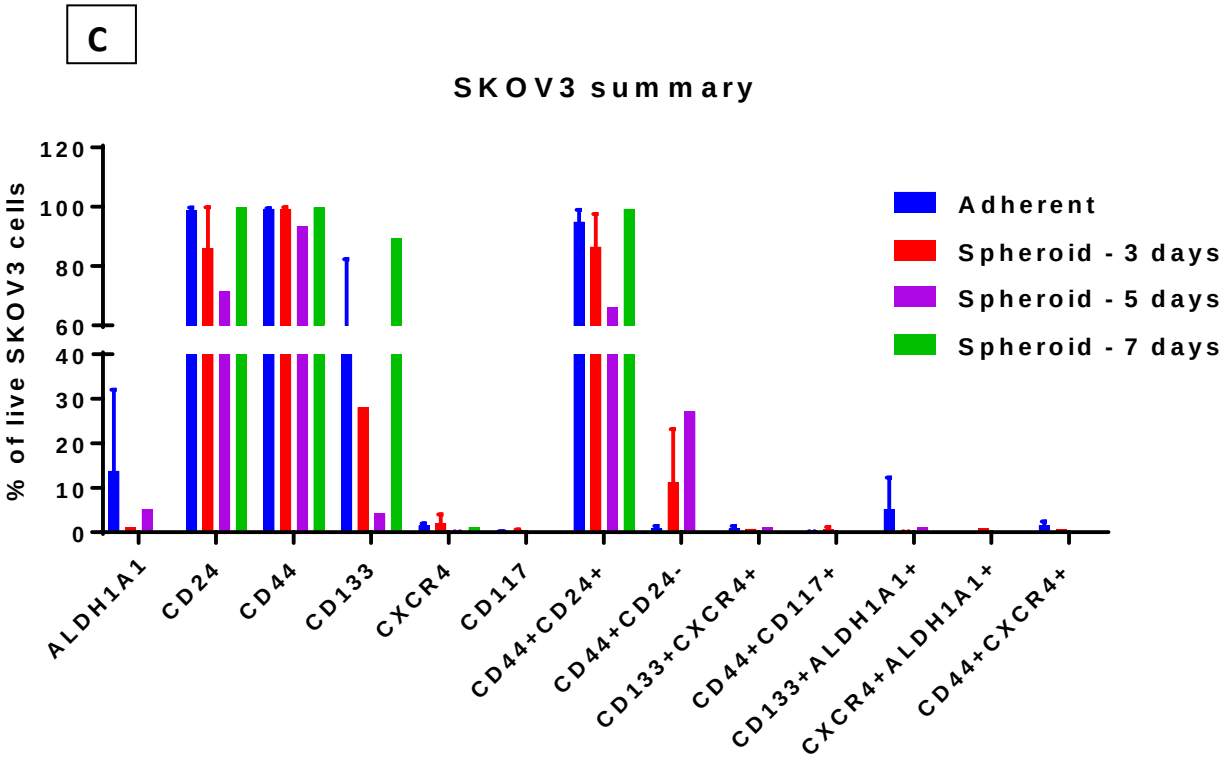

Fig22. Surface marker analysis and sphere formation assay to identify potential stem cell markers for all the cell lines shown below. A) SKOV3 grown under adherent and non-adherent conditions shows the relative expression of marker candidates for stem cells. B) Shows the non-adherent phenotype taken on different days and C) Shows the expression levels marker candidates for stem cells harvested on different days.

A.

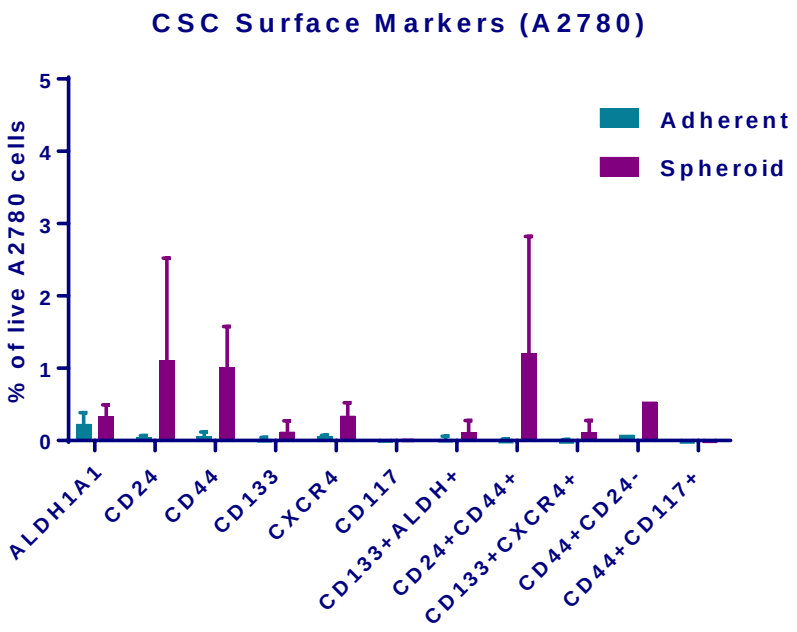

B.

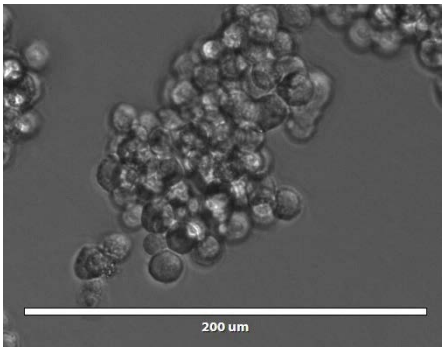

C.

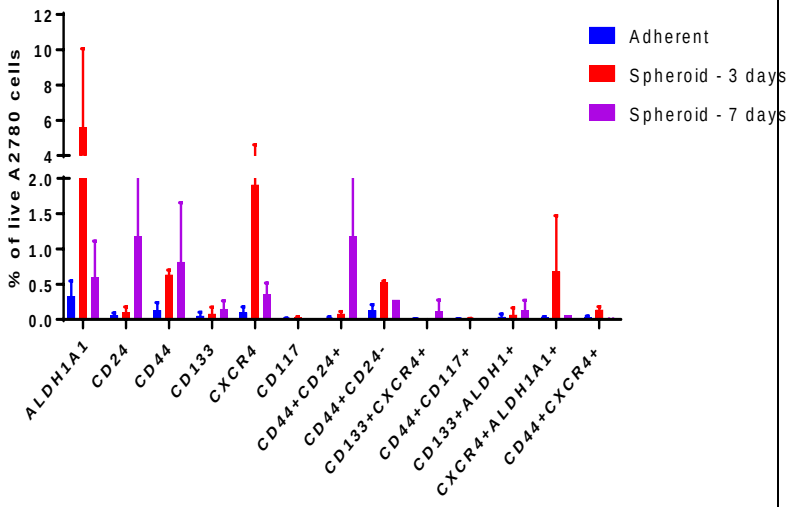

Fig23. Surface marker analysis and sphere formation assay to identify potential stem cell markers for all the cell lines shown below. A) A2780 grown under adherent and non-adherent conditions shows the relative expression of marker candidates for stem cells. B) Shows the non- adherent phenotype taken on different days and C) Shows the expression levels marker candidates for stem cells harvested on different days.

A.

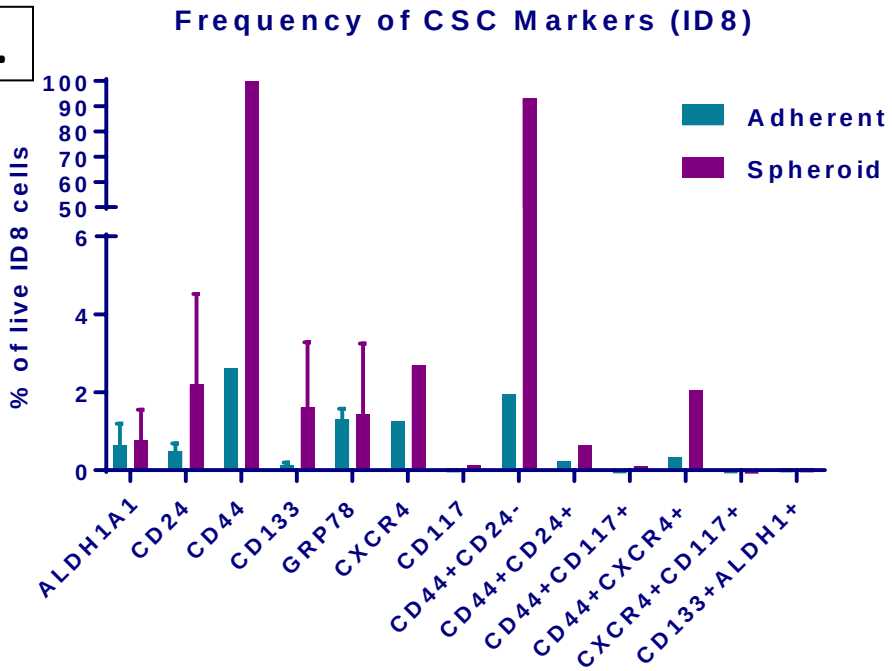

B.

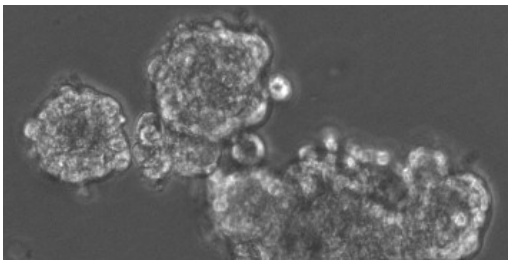

7 day culture (10x)

C.

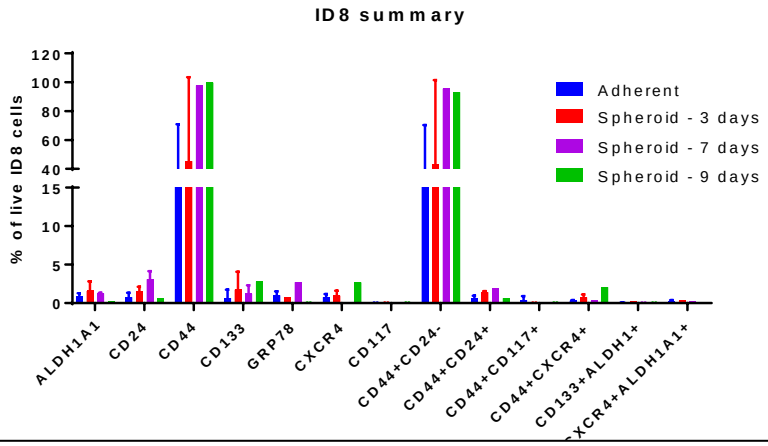

Fig24. Surface marker analysis and sphere formation assay to identify potential stem cell markers for all the cell lines shown below. A) ID8 grown under adherent and non-adherent conditions shows the relative expression of marker candidates for stem cells. B) Shows the non- adherent phenotype taken on different days and C) Shows the expression levels marker candidates for stem cells harvested on different days

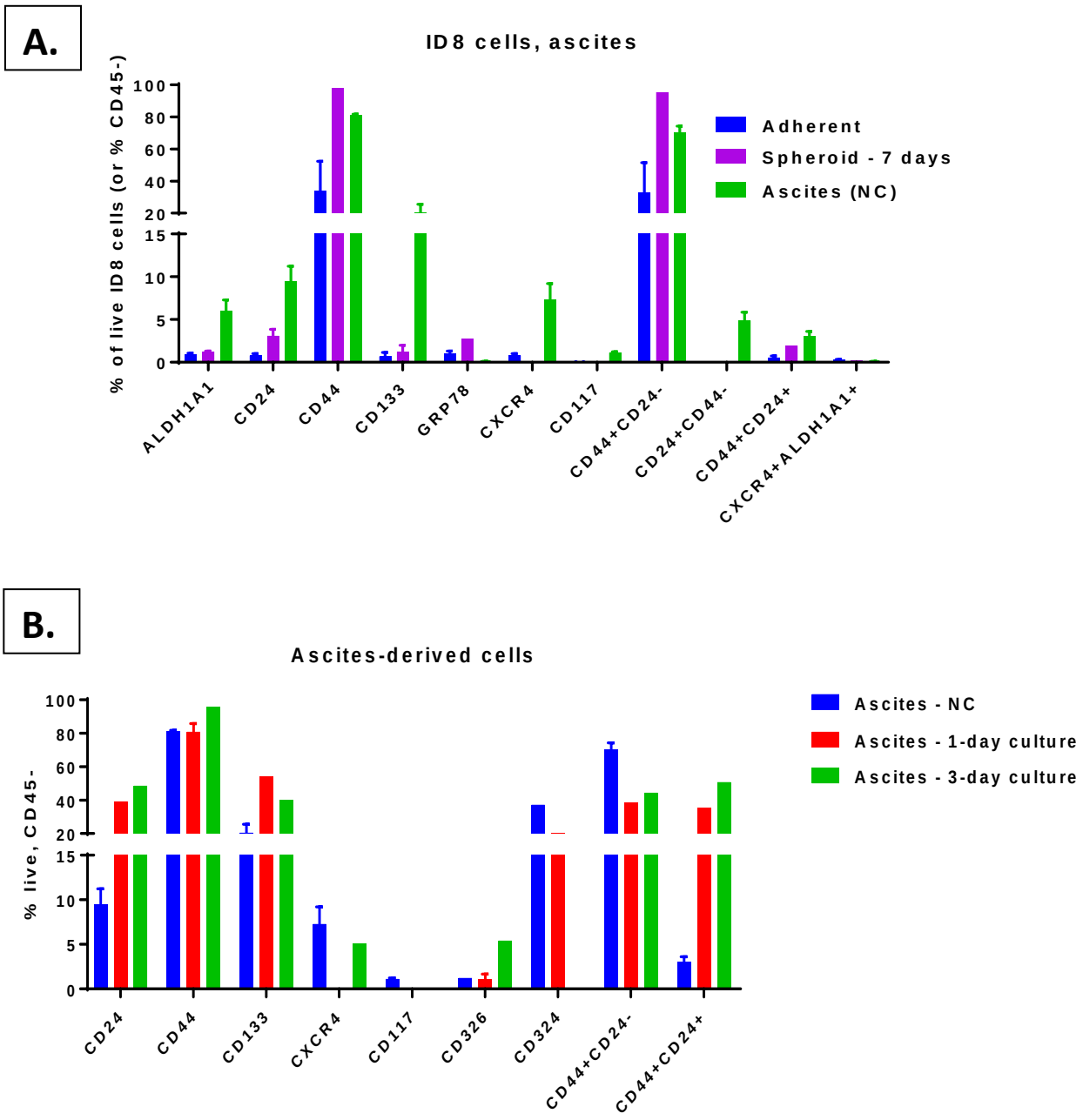

Fig25: Surface marker analysis and sphere formation assay to identify potential stem cell markers for all the cell lines shown below. A) ID8 grown under adherent and non-adherent conditions were compared with the tumors isolated from ascites showing the relative expression of marker candidates for stem cells. B) Ascites were cultured on different days in suspension culture and relative expression levels of different candidate markers are shown.

STEM CELLS ENRICHMENT USING CHEMOTHERAPY BASED TREATMENT

CSCs selected in culture by treatment with paclitaxel to aid in expansion of CSCs in ovarian cancer cell lines. Treatment of cells with 20uM of paclitaxel for 72 hours followed by non-adherent culture conditions demonstrated enrichment of spheroids.

PACLITAXEL TREATMENT

		72 hour harvest			
	Plated	NT- count	NT - viability	Pac+ count	Pac+ viability
ID8	3.00E+05	7.70E+06	96%	4.99E+05	89%
ID8-F3	3.00E+05	7.80E+06	93%	6.60E+05	63%
SKOV3	6.00E+05	1.40E+06	100%	2.99E+05	53%
A2780	3.00E+05	3.80E+06	99%	7.60E+04	65%

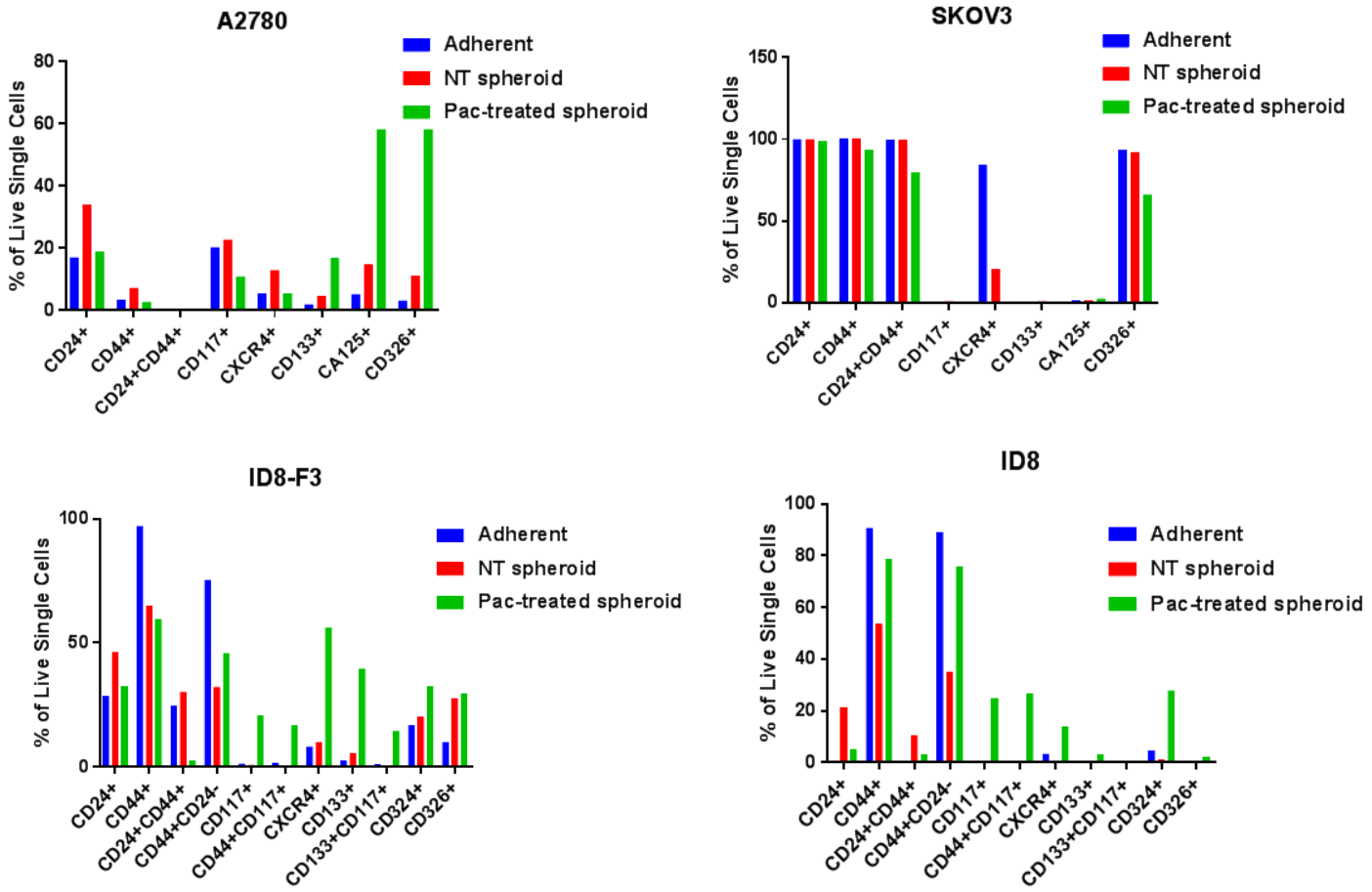

Fig26. Selection of potential Cancer stem cell markers- Four cell lines (A2780, SKOV3, ID8 and ID8-F3) were subjected to paclitaxel treatment for 72 hours and the resulting cells were cultured for additional 3 days in suspension. These cells were then stained for different CSCs markers and compared with non-treated cells in adherent and suspension settings.

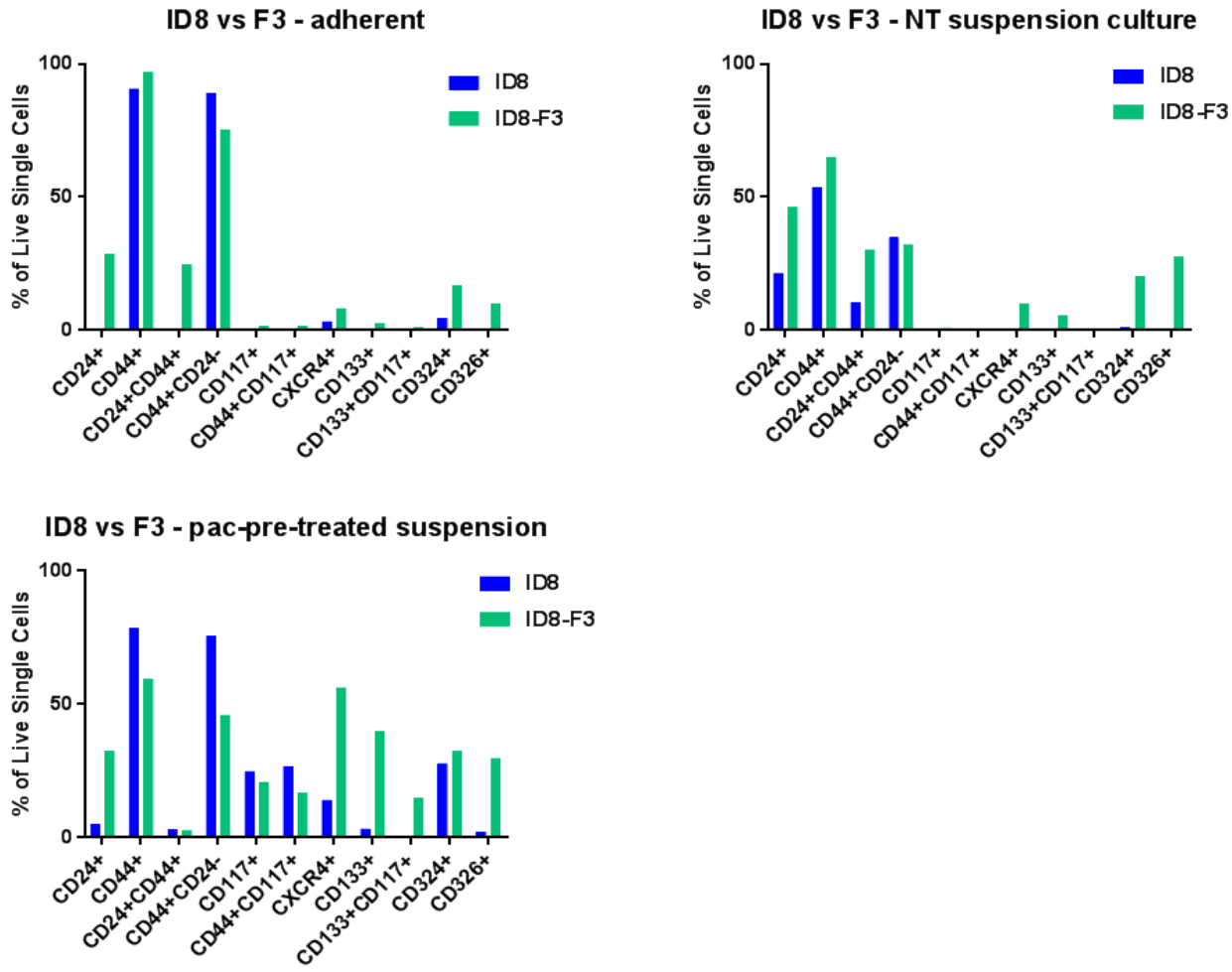

Fig27. Comparison between ID8 and ID8-F3 cancer stem cell markers- These two cell lines were compared in culture condition to evaluate potential stem cell markers in vitro.

A. **Enrichment of Cancer stem cells with suspension culture**

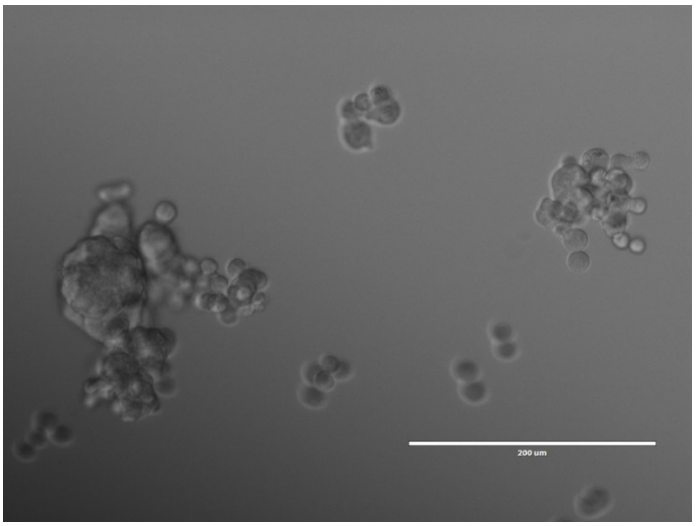

14 Day culture- 10X

B. **qRT-PCR on ID8-F3 Adherent and ID8-F3 Spheroid Unsorted)**

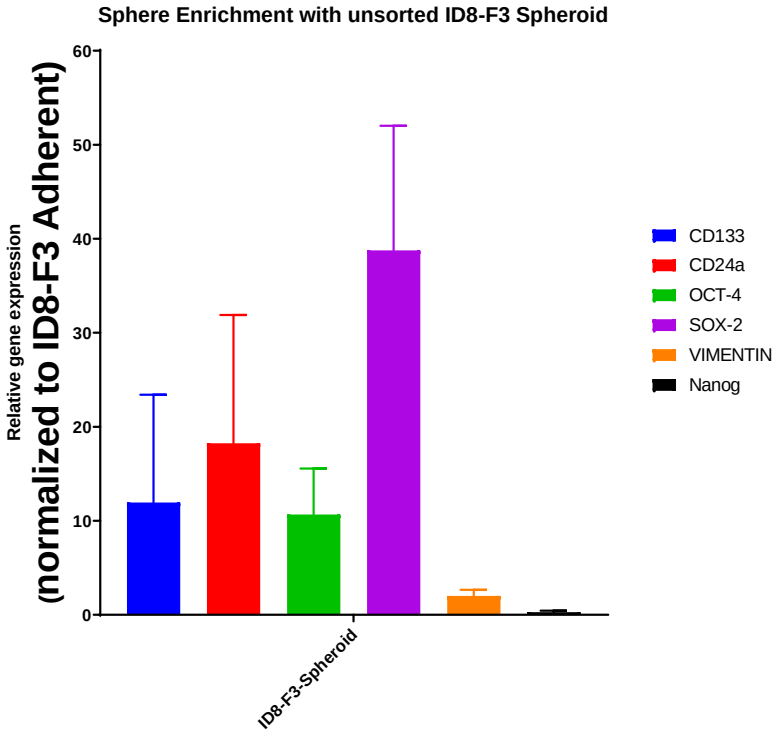

C. **qRT-PCR on ID8-F3 Adherent and ID8-F3 Spheroid (Sorted)**

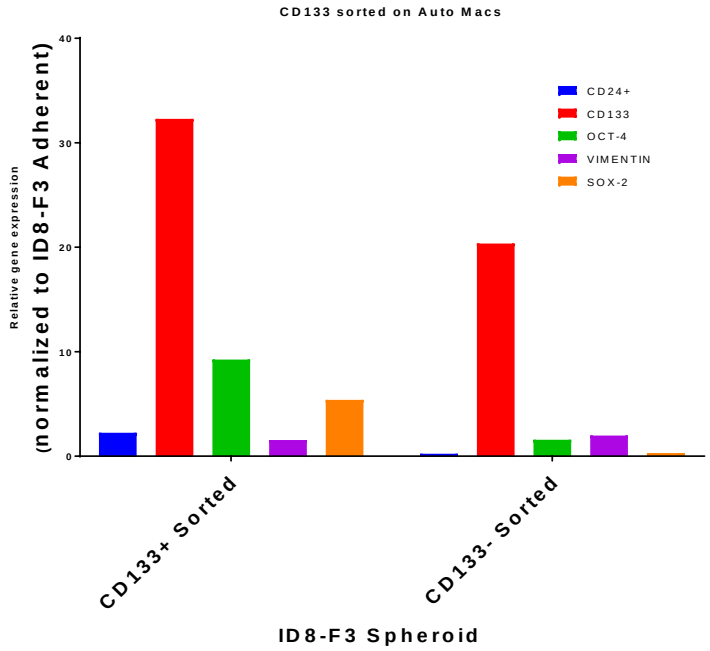

D.

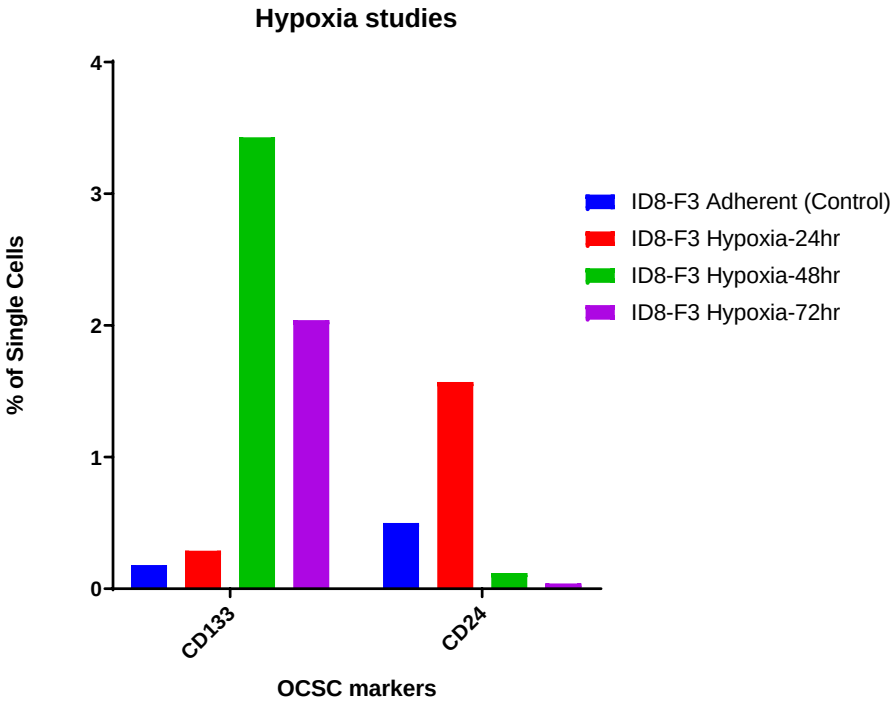

Fig28. A) ID8-F3 cells in suspension- ID8-F3 cells were grown in suspension culture for enriching the cancer stem cells. This is a Day-14 image taken by Evos fluorescent microscope at 10X magnification. B) **Relative gene expression-** qRT-PCR on ID8-F3 cells grown in adherent condition and ID8-F3 spheroids grown in suspension medium were profiled to see the relative stemness (n=3). C) **Comparison of gene expression-** Comparing the relative stemness using qRT-PCR. between the ID8-F3 cells grown in adherent condition and ID8-F3 spheroids grown in suspension condition and sorted for CD133 +/- via Auto Macs Pro separator. D) **Hypoxia studies-** Shows the hypoxic microenviroment upgrades stem-like properties of ovarian cancer cells.

Reportable outcomes Aim 3, Experiment 1: The stem cell markers for all four cell lines (two murine and two human) mentioned above have been evaluated using sphere formation assay and chemotherapy based treatments. A number of potential cancer stem cell markers have been identified (CD133+, CA125+ and CD326+) which are investigated downstream in a mouse cell line. We saw distinguishable increase in CD133+ and CD24+ in the ID8-F3 model (Fig27) with paclitaxel treatment. We validated the stemness expression in suspension cultures grown over extended period in cultures (chemotherapy based treatment were stopped as it changes the phenotype and cell line characteristics). We cultured ID8-F3 cells in adherent condition and spheroids in suspension cultures for 14 days and the spheroid cells were harvested and sorted using anti-CD133 magnetic beads via Auto Macs Pro Separator. Sorted cells were then compared by normalizing with the adherent cells using qRT-PCR. and we saw increased CD133+ fractions in the suspension cultures (Fig 28D). These sorted cells were also tested for potential stemness related genes like Vimentin, Nanog, Sox2 and Oct4. Interestingly, we identified an increase in CD24 (Fig28B) which is also a candidate cancer stem cell marker [18]. Moreover, the non-sorted cells from both adherent and suspension cells showed the same trend of fold change in stem cell markers and their respective phenotypes (Fig28-B and C). Furthermore, the expression of the cancer stem cell phenotype was analyzed using hypoxia studies (Fig24D) which confirms similar findings [19] at different time points. RNA isolation was done for the ID8-F3 adherent and enriched unsorted spheroids from suspension cultures which will be sent for RNA sequencing to find potential antigens that can be cloned into a suitable vector for DNA vaccination based on the pVax vector system (Life Technologies).

Aim 3, Experiment 2: The antigens derived from Experiment 1 will be assessed for their ability to suppress tumor growth. We will use tumor cell lines transplanted into syngeneic mice. Mice will be immunized with antigen-encoding pVax1 vaccine. The vaccine's ability to suppress tumor growth will be determined by measuring tumor burden at 70 days. A 25% reduction in tumor growth will be considered evidence of a tumor rejecting antigen. We anticipate 20 immunogenic antigens from Experiment 1, a Poly I:C control group and a mock-treated control group will also be included. This experiment is not started.

Aim 3, Experiment 3**.** We expect to identify a total of 6 antigens (3 from epithelial tumor cells and 3 from cancer stem cells). Our goal for this experiment is to derive a combination of 4 antigens (2 from each cell type) that block tumor growth better than best antigen identified in Experiment 2. We will again use tumor cell lines transplanted into syngeneic mice. The vaccine's ability to suppress tumor growth will be determined by measuring tumor burden at 70 days. We will use 9 mice per group and have 9 groups, each receiving different combinations of 4 antigens, and 4 controls (epithelial tumor cell antigens-only, cancer stem cell antigens-only, Poly I:C control, mock vaccinated control), for a total of 13 groups. This experiment is not started.

Aim 3, Experiment 4**.** Determine if T cell priming with vaccine enhances efficacy of PD-1 blockade. In this experiment we will integrate the results from Aims 1 and 2. For this experiment, we expect to have a multi-antigen DNA vaccine that targets both epithelial tumor cells as well as ovarian CSCs. The final vaccine preparation will consist of an equimolar mixture of 4 distinct plasmids that will be administered with the most efficacious adjuvant identified in Experiment 1 above. The hypothesis to be tested is that a multi-antigen DNA vaccine targeting antigens with relevance in human ovarian cancer will prime the immune system to respond better to PD-1 blockade resulting in long term durable remissions. All mice (C57BL/6) will be injected with $5x10^6$ ID8 cells in a volume of 500µL normal saline [15]. Mice will receive immunization with the vaccine on day 7, followed by boosters on days 9 and 11. On day 18, mice will receive anti-PD-1 therapy (11 doses, every 3 days). Seven days after last anti-PD-1 dose, we will euthanize the mice and collect tissues for immunologic analyses. Spleens will be collected and used to measure presence of immune effector cells by ELISpot analysis. Tumor weights will be compared among the groups as well. Mice receiving combination therapy of vaccine and anti-PD-1 will be compared to controls and those groups receive either vaccine or anti-PD-1 alone. This experiment is not started.

The Key Research Accomplishments

- Developed flow panels for different immune cell subsets associated with ovarian cancer microenvironment.
- Demonstrated the influence of IL-10 in upregulating the PD-1 expression upon anti-PD-1 treatment in tumor bearing mice.
- Demonstrated significant reduction in tumor burden and increased survival in tumor bearing mice upon anti-PD-1 and anti-IL-10 combination treatment.
- Identified several ovarian cancer stem cell markers by enriching different ovarian cancer cell lines in suspension culture.

Reportable outcomes:

1. **IL-10 is significantly increased in tumor bearing mice upon anti-PD-1 treatment.**
2. **IL-10 plays a vital role in suppressing immune cells in ovarian cancer tumor microenvironment.**
3. **Combination treatment with anti-PD-1 and anti-IL-10 in tumor bearing mice significantly reduces tumor burden and improves scope for immunoediting.**
4. **CD133+ and CD24a+ in ID8-F3 cell line were identified as potential stem cell markers in mouse ovarian cancer**

Publications:

IL10 Release upon PD-1 Blockade Sustains Immunosuppression in Ovarian Cancer.
Lamichhane P, Karyampudi L, Shreeder B, Krempski J, Bahr D, Daum J, Kalli KR, Goode EL, Block MS, Cannon MJ, Knutson KL.
https://www.ncbi.nlm.nih.gov/pmc/articles/PMC5712245/

CONCLUSION- PD-1/PD-L1 axis is a part of major immune suppressive network. Blocking this axis leads to enhancement of other immune suppressive mechanism. Our goal is to identify different immune suppressive modulators in ovarian cancer microenvironment. Based on this information we aim to develop strategies to regulate systemic and local immune responses. On the contrary cancer stem cells also play a vital role in tumor recurrence and morbidity. A deeper level of understanding on the mechanism by which the cancer stem cells evades the tumor microenvironment is critical to eradicate ovarian cancer.

REFERNCES:

1. Zhang, L., J.R. Conejo-Garcia, D. Katsaros, P.A. Gimotty, M. Massobrio, G. Regnani, A. Makrigiannakis, H. Gray, K. Schlienger, M.N. Liebman, S.C. Rubin, and G. Coukos, *Intratumoral T cells, recurrence, and survival in epithelial ovarian cancer.* N Engl J Med, 2003. **348**(3): p. 203-13 http://www.ncbi.nlm.nih.gov/pubmed/12529460.
2. Hamanishi, J., M. Mandai, M. Iwasaki, T. Okazaki, Y. Tanaka, K. Yamaguchi, T. Higuchi, H. Yagi, K. Takakura, N. Minato, T. Honjo, and S. Fujii, *Programmed cell death 1 ligand 1 and tumor-infiltrating CD8+ T lymphocytes are prognostic factors of human ovarian cancer.* Proc Natl Acad Sci U S A, 2007. **104**(9): p. 3360-5 http://www.ncbi.nlm.nih.gov/pubmed/17360651.
3. Josephine Walton, Julianna Blagih, Darren Ennis1, Elaine Leung, Suzanne Dowson1, Malcolm Farquharson, Laura A. Tookman, Clare Orange, Dimitris Athineos, Susan Mason, David Stevenson, Karen Blyth, Douglas Strathdee, Frances R. Balkwill, Karen Vousden, Michelle Lockley, and Iain A. McNeish) (CRISPR/Cas9-Mediated Trp53 and Brca2 Knockout to Generate ImprovedMurineModels of Ovarian High-Grade Serous Carcinoma DOI: 10.1158/0008-5472.CAN-16-1272 https://www.ncbi.nlm.nih.gov/pubmed/27530326\
4. Gabrilovich, D.I. and S. Nagaraj, *Myeloid-derived suppressor cells as regulators of the immune system.* Nat Rev Immunol, 2009. **9**(3): p. 162-74 http://www.ncbi.nlm.nih.gov/pubmed/19197294.
5. Lan, C., X. Huang, S. Lin, H. Huang, Q. Cai, T. Wan, J. Lu, and J. Liu, *Expression of M2-polarized macrophages is associated with poor prognosis*

for advanced epithelial ovarian cancer. Technol Cancer Res Treat, 2013. **12**(3): p. 259-67 http://www.ncbi.nlm.nih.gov/pubmed/23289476.

6. Krockenberger, M., Y. Dombrowski, C. Weidler, M. Ossadnik, A. Honig, S. Hausler, H. Voigt, J.C. Becker, L. Leng, A. Steinle, M. Weller, R. Bucala, J. Dietl, and J. Wischhusen, *Macrophage migration inhibitory factor contributes to the immune escape of ovarian cancer by down-regulating NKG2D.* J Immunol, 2008. **180**(11): p. 7338-48 http://www.ncbi.nlm.nih.gov/pubmed/18490733.
7. Hamanishi, J., M. Mandai, M. Iwasaki, T. Okazaki, Y. Tanaka, K. Yamaguchi, T. Higuchi, H. Yagi, K. Takakura, N. Minato, T. Honjo, and S. Fujii, *Programmed cell death 1 ligand 1 and tumor-infiltrating CD8+ T lymphocytes are prognostic factors of human ovarian cancer.* Proc Natl Acad Sci U S A, 2007. **104**(9): p. 3360-5 http://www.ncbi.nlm.nih.gov/pubmed/17360651.
8. Nuti, S.V., G. Mor, P. Li, and G. Yin, *TWIST and ovarian cancer stem cells: implications for chemoresistance and metastasis.* Oncotarget, 2014. **5**(17): p. 7260-71 http://www.ncbi.nlm.nih.gov/pubmed/25238494.
9. Shah, M.M. and C.N. Landen, *Ovarian cancer stem cells: are they real and why are they important?* Gynecol Oncol, 2014. **132**(2): p. 483-9 http://www.ncbi.nlm.nih.gov/pubmed/24321398.
10. Yan, H. and Y. Sun, *Evaluation of the mechanism of epithelial-mesenchymal transition in human ovarian cancer stem cells transfected with a WW domain-containing oxidoreductase gene.* Oncol Lett, 2014. **8**(1): p. 426-430 http://www.ncbi.nlm.nih.gov/pubmed/24959289.
11. Cioffi, M., C. D'Alterio, R. Camerlingo, V. Tirino, C. Consales, A. Riccio, C. Ierano, S.C. Cecere, N.S. Losito, S. Greggi, S. Pignata, G. Pirozzi, and S. Scala, *Identification of a distinct population of CD133(+)CXCR4(+) cancer stem cells in ovarian cancer.* Sci Rep, 2015. **5**: p. 10357 http://www.ncbi.nlm.nih.gov/pubmed/26020117.
12. Long, H., T. Xiang, W. Qi, J. Huang, J. Chen, L. He, Z. Liang, B. Guo, Y. Li, R. Xie, and B. Zhu, *CD133+ ovarian cancer stem-like cells promote non-stem cancer cell metastasis via CCL5 induced epithelial-mesenchymal transition.* Oncotarget, 2015. **6**(8): p. 5846-59 http://www.ncbi.nlm.nih.gov/pubmed/25788271.
13. Wang, X., X. Li, X. Fu, M. Bai, Q. Mei, J. Nie, Z. Wu, and W. Han, *Eliminating ovarian cancer stem cells: a potential therapeutic target for ovarian cancer chemoresistance.* Curr Protein Pept Sci, 2015. **16**(4): p. 270-8 http://www.ncbi.nlm.nih.gov/pubmed/25929861.
14. Zhang G, L Ma, YK Xie, XB Miao and C Jin. (2012). Esophageal cancer tumorspheres involve cancer stem-like populations with elevated aldehyde dehydrogenase enzymatic activity. Mol Med Report 6:519–524.
15. Krempski J, Karyampudi L, Behrens MD, Erskine CL, Hartmann L, Dong H, Goode EL, Kalli KR, Knutson KL. Tumor-infiltrating programmed death receptor-1+ dendritic cells mediate immune suppression in ovarian cancer. J Immunol. 2011 Jun 15;186(12):6905-13. doi:10.4049/jimmunol.1100274. Epub 2011 May 6. https://www.ncbi.nlm.nih.gov/pubmed/21551365

16. Curiel TJ, Wei S, Dong H, Alvarez X, Cheng P, Mottram P, Krzysiek R, Knutson KL, Daniel B, Zimmermann MC, David O, Burow M, Gordon A, Dhurandhar N, Myers L, Berggren R, Hemminki A, Alvarez RD, Emilie D, Curiel DT, Chen L, Zou W. Blockade of B7-H1 improves myeloid dendritic cell-mediated antitumor immunity. Nat Med. 2003 May;9(5):562-7. Epub 2003 Apr 21. https://www.ncbi.nlm.nih.gov/pubmed/12704383

17. Jiang-jie Duan, Wen Qiu, Sen-lin Xu, Bin Wang, Xian-zong Ye, Yi-fang Ping, Xia Zhang, Xiu-wu Bian, and Shi-cang Yu Strategies for Isolating and Enriching Cancer Stem Cells: Well Begun Is Half Done https://www.ncbi.nlm.nih.gov/pmc/articles/PMC3730373/

18. Chun-Hung Yang, Hui-Ling Wang, Yi-Sheng Lin, K. P. Shravan Kumar, Hung-Chi Lin, Chih-Jung Chang, Chia-Chen Lu , Tsung-Teng Huang, Jan Martel , David M. Ojcius, Yu-Sun Chang, John D. Young, Hsin-Chih Lai Identification of CD24 as a Cancer Stem Cell Marker in Human NasopharyngealCarcinoma https://journals.plos.org/plosone/article/metrics?id=10.1371/journal.pone.0099412

19. Pan Wang,[1] Wen-wu Wan,[1] Shuang-Long Xiong,[2] Hua Feng,[1] and Nan Wu Cancer stem-like cells can be induced through dedifferentiation under hypoxic conditions in glioma, hepatoma and lung cancer https://www.ncbi.nlm.nih.gov/pmc/articles/PMC5253691/